Article

Not peer-reviewed version

# Preparation of Mono- and Bivalent (Bis) Prostate-Specific Membrane Antigen (PSMA) Ligands and Their Preclinical Investigation as PET Imaging Agents for PSMA-Receptor Positive Prostate Cancer

Subhani M. Okarvi *

Posted Date: 14 April 2026

doi: 10.20944/preprints202604.0979.v1

Keywords: PSMA; PSMA receptors; PSMA ligands; preclinical evaluation; tumor targeting

 doi:10.20944/preprints202604.0979.v1



*Article*

# Preparation of Mono- and Bivalent (Bis) Prostate-Specific Membrane Antigen (PSMA) Ligands and Their Preclinical Investigation as PET Imaging Agents for PSMA-Receptor Positive Prostate Cancer

**Subhani M. Okarvi**

Cyclotron and Radiopharmaceuticals Department. Innovation and Research. King Faisal Specialist Hospital and Research Centre. MBC 03, P.O. Box 3354, Riyadh 11211, Saudi Arabia; sokarvi@kfshrc.edu.sa

**Abstract**

Prostate-specific membrane antigen (PSMA) targeting radiopharmaceuticals have been successfully used for the diagnosis and therapy of prostate cancer. Most of the PSMA molecules for the diagnosis and treatment are based on the peptidomimetic glutamate-urea-lysine (Glu-CO-Lys) pharmacophore connected to various linker groups. Optimization of the available agents is desirable to improve tumor uptake and reduce uptake in non-target organs. This can be achieved, for instance, via linker modifications and/or multivalent approaches. In this study, we synthesized several new Glu-CO-Lys-based PSMA ligands, each connected to different linkers to explore the role of these linkers on cell binding and tumor targeting potential. Additionally, a bivalent (bis) PSMA ligand, containing two PSMA targeting motifs (Glu-CO-Lys) in the same structure, was synthesized by conventional Fmoc-based solid-phase synthesis. DOTA- or Aoa-coupled PSMA conjugates showed high radiolabeling efficiency (≥ 90%) with [$^{68}$Ga] and [$^{18}$F] and resulted in the formation of one major radiolabeled product. Also, a high stability of the PSMA conjugates was found in human plasma. The [$^{68}$Ga/$^{18}$F]-labeled PSMA ligands exhibited the nanomolar affinity (<95 nM) specific to the PSMA-positive LNCaP tumor cell line. In the PSMA-positive tumor xenograft model, the radiolabeled PSMA ligands exhibited rapid clearance from the blood and excretion primarily via the renal system. Biodistribution and imaging studies revealed high accumulation of bis-PSMA ligand in LNCaP tumor xenografts. These render that bis-PSMA may be a promising ligand for diagnostic imaging of PSMA-positive prostate cancer.

**Keywords:** PSMA; PSMA receptors; PSMA ligands; preclinical evaluation; tumor targeting

## 1. Introduction

Despite recent advancements in nuclear medical imaging and radionuclide therapy, prostate cancer (PCa) remains the most frequently diagnosed cancer type in men and is estimated to be the fifth leading cause of cancer-related deaths in men worldwide [1]. Patients who are diagnosed with prostate cancer at later stages usually have poor treatment outcomes, emphasizing the necessity for early and accurate detection and ultimately better treatment options for prostate cancer patients. Prostate-specific membrane antigen (PSMA) is a type II transmembrane glycoprotein, overexpressed in about 90% of prostate cancer cases, while its expression on healthy tissues is low, making it an excellent clinically-relevant molecular target for diagnostic imaging and radionuclide therapy of prostate cancer. Furthermore, binding of a PSMA targeting agent to the active center of the extracellular domain of PSMA generally leads to internalization in the cancer lesion and ultimately enhanced retention in the cancer cells [2]. Due to these distinct properties, PSMA constitutes a useful molecular marker and ideal target for imaging and therapy of PCa. Given its high PSMA expression in almost all human prostate cancer types and further enhancement of its expression in poorly

 doi:10.20944/preprints202604.0979.v1



differentiated, metastatic, and hormone-refractory carcinomas, there has been a high clinical interest in developing potent PSMA-specific radiopharmaceuticals for precise diagnosis, staging, and treatment of prostate carcinoma. In addition, PSMA can be used as a vehicle to carry cytotoxic drugs specifically to prostate cancer cells, with low damage to adjacent healthy cells [3–5]. A general design for the development of PSMA-targeted radiopharmaceuticals is presented in Figure 1.

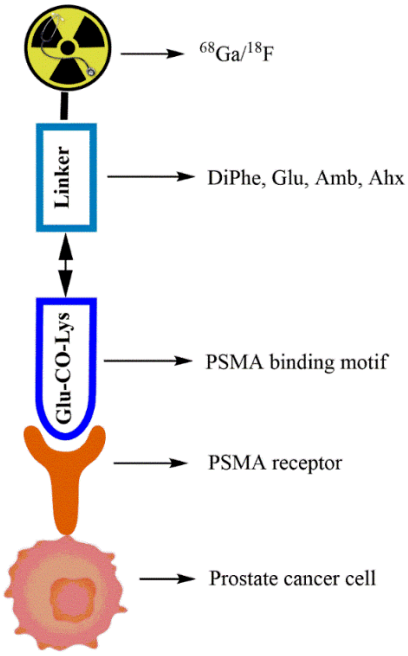


**Figure 1.** General design of PSMA-targeted radiopharmaceutical.

PSMA-receptor targeting molecules are radiopharmaceuticals that specifically bind to PSMA, a protein highly expressed in prostate cancer, for both diagnostic imaging and radionuclide therapy. Until now, a wide variety of PSMA-targeting agents have been described, varying from intact antibodies to low-molecular-weight compounds. Small biomolecules exploit the binding of substrates, including folate hydrolase 1, N-acetylated $\alpha$-linked acidic dipeptidase (NAALADase), or glutamate carboxypeptidase II, to the active site of PSMA [4,6]. In recent years, numerous compounds based on glutamate-urea-lysine (Glu-NH-CO-NH-Lys, Figure 2) PSMA-binding motifs have been developed [2,3]. Some clinically useful PSMA-PET imaging agents include [$^{68}$Ga]Ga-PSMA-11 and [$^{18}$F]-DCFPyL, which detect the cancer, and radionuclide therapies, such as [$^{177}$Lu]Lu-PSMA-617, which deliver radiation to PSMA-positive tumors to treat metastatic prostate cancer. These radioligands enable a "theranostic" approach, combining diagnosis and therapy. Recently, two of the PSMA compounds gained US-FDA approval [3,6–8]. Although many PSMA-based ligands have been prepared and evaluated, there is still room for the development of potent PSMA ligands with better pharmacokinetic properties, especially in terms of low uptake in the liver, intestines, and kidneys [6,9,10].

 doi:10.20944/preprints202604.0979.v1



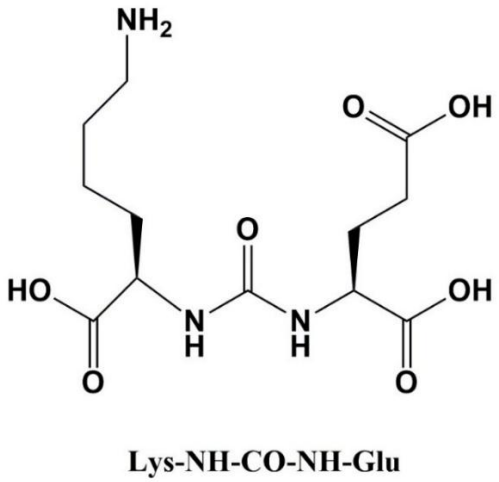


**Figure 2.** Chemical structure of the PSMA binding motif, lysine-urea-glutamate.

In recent years, much focus has been on the development of personalized medicine in nuclear oncology, where radiopharmaceutical therapies are tailored to the particular characteristics of the individual patient and the tumor. In prostate cancer, there is increasing evidence that PSMA may be a potential target for both diagnostic imaging and targeted radionuclide therapy. Furthermore, modifying the imaging agent by replacing the diagnostic radionuclide with a therapeutic one allows delivery of high doses of lethal radiation to specific tumor sites. This "diagnosis and therapy" based theranostic strategy holds great clinical potential as an effective treatment modality in managing prostate cancer [11,12]. Due to the recent developments in radiopharmaceutical chemistry, nuclear imaging modalities, and technologies, molecular imaging now plays a vital role in personalized cancer management, as it aims to deliver patient-specific targeted treatment at the appropriate time to maximize the therapeutic outcomes. Two frequently used molecular imaging modalities for diagnosis or image-based guided therapy of cancer are single-photon emission computed tomography (SPECT) and positron emission tomography (PET) using radiolabeled compounds. SPECT and PET are highly sensitive, noninvasive medical technologies that can measure tumor receptor expression for the entire tumor burden and provide highly sensitive images of cancer lesions, thus avoiding the sampling error that may occur with heterogeneous tumor receptor expression. Owing to the substantial biological and clinical heterogeneity of prostate cancer, molecular imaging, especially with PET, has shown its usefulness in efficient targeting of this prevalent disease [2].

It has been well described that the linker groups play vital roles in determining the fate of biological as well as tumor-targeting properties of peptides and peptidomimetics. The careful selection of a linker capable of enhancing the binding and biological activity of PSMA targeting is important [9,10,13–15]. To determine the effect of the nature of the chelate and the length and composition of the linker on binding affinity, we focused in this study, towards the developing PSMA analogs in which amino acids, such as DiPhe, Glu, Ahx or Amb are linked to Glu-urea-Lys binding core to improve binding and tumor targeting characteristics as well as to enhance renal excretion of PSMA specific ligands. These diverse linkers are selected because of their ease of synthesis and conjugation by solid-phase synthesis to the PSMA binding motif. Based on the structure of PSMA-617 (Figure 3), seven analogs, with different linkers, were designed and synthesized, with the general structure of Glu-urea-Lys-X- DOTA/Aoa, where X was the position of substitution and/or addition of linker groups (Scheme 1).

 doi:10.20944/preprints202604.0979.v1



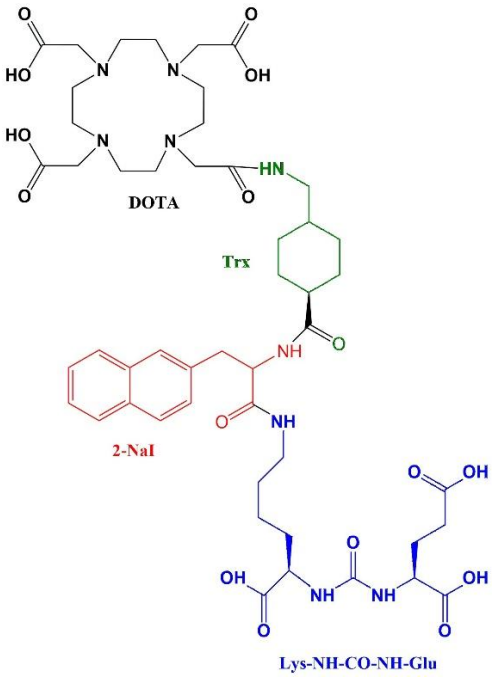


**Figure 3.** Chemical structure of DOTA-PSMA-617.

Mono- and bis-PSMA ligands differ in their structure and function: monomers are single-unit molecules with a single binding site, while dimers are two-unit molecules with two binding sites. The monomeric PSMA ligands are small molecules and are more suitable for early diagnostic imaging because of their rapid pharmacokinetics, making them ideal for diagnostic imaging with short-lived radionuclides, such as [$^{68}$Ga] and [$^{18}$F]. On the other hand, the bis-PSMA ligands can lead to increased tumor uptake and retention through the multivalency effect [6,16–19]. While monovalent ligands, such as PSMA-617, are already approved and widely used, newer bis-PSMA compounds, such as SAR-bisPSMA, are currently being evaluated in clinical trials to confirm these potential benefits in patients. Recently, it has been shown that the [$^{64}$Cu]-SAR-bisPSMA demonstrated 2-3 times higher tumor uptake, prolonged retention, and detection of additional prostate cancer lesions compared to approved PSMA agents [19,20].

Herein, we present the design, synthesis, and preclinical evaluation of eight PSMA-binding radioligands with structural modifications of the linker groups connected to either DOTA radiometal chelator for radiolabeling with [$^{68}$Ga] or Aoa aminooxy group for radiolabeling with [$^{18}$F]. Additionally, we have also synthesized a bivalent (bis) PSMA ligand, containing two PSMA targeting motifs (Glu-urea-Lys) in one construct, to explore its effectiveness over the corresponding mono PSMA ligand. The synthesis, radiolabeling with [$^{68}$Ga] and [$^{18}$F], and in vitro and in vivo evaluation are described in this research paper.

## 2. Materials and Methods

*General*

All analytical grade chemicals and Fmoc-protected amino acids with appropriate side-chain protections were purchased from commercial sources and used without further purification. DOTA-tris-(t-Bu ester) was bought from Chematech, France. The structural identities of each newly synthesized PSMA molecule were confirmed by mass spectrometry performed on an Agilent 6125 single quadrupole liquid chromatography/mass spectrometry system (LC/MS) (Agilent Technologies, Santa Clara, CA, USA) using an eluent of 0.1% formic acid/29.95% $H_2O$/69.95% $CH_3CN$ at a flow rate of 0.3 mL/min. Reversed-phase high-performance liquid chromatography (RP-HPLC) analyses were performed on a Shimadzu HPLC system (Shimadzu Corporation, Kyoto, Japan) fitted with a dual-wavelength UV-VIS detector (Shimadzu Corporation, Kyoto, Japan), a radioactivity

 doi:10.20944/preprints202604.0979.v1



detector (Bioscan, USA), and the Lauralite chromatogram analysis software (LabLogic Systems Ltd., Sheffield, UK). Radioactive samples were measured by using a γ-counter (Mucha, Raytest Isotopenmessgeräte GmbH, Straubenhardt, Germany).

**1. Synthesis of PSMA-binding motif (Glu-NH-CO-NH-Lys)**

The synthetic steps for the preparation of the PSMA binding motif are depicted in Scheme 1.

In a first step, the isocyanate of the glutamate moiety **2** was generated in situ. For this, a solution of 1 mmol triphosgene in 5 mL dry DCM (dichloromethane) was cooled in an ice bath (0–4° C). To this, 3 mmol H-Glu-(OtBu)-OtBu.HCl **1** dissolved in 150 mL of DCM, and 2.5 mL of DIPEA (*N*,*N*-Diisopropylethylamine) were added dropwise over 3–4 h, while maintaining the reaction temperature below 4° C. The reaction mixture was further stirred for 1 h at room temperature. The isocyanate of glutamate moiety **2** was then mixed with 0.3 mmol of $NH_2$-Lys(Alloc)-resin **4** (prepared separately by removing the Fmoc group of Fmoc-$NH_2$-Lys(Alloc)-wang resin **3**), and the reaction mixture was stirred at room temperature for 16 h. The solvent was drained, and the resin was washed with DMF (dimethylformamide) and DCM. The Alloc protecting group from epsilon amino group of lysine was then removed by treating with a mixture of 100 mg tetrakis(triphenylphosphine)palladium(0) in 3 mL DCM and 300 µL morpholine for 2 h in the dark. The procedure was repeated twice. The resin was washed several times with 1% DIPEA in DMF (v/v), followed by washing with 2% sodium diethylthiocarbamate in DMF to remove residual palladium and to provide Glu-NH-CO-NH-Lys–resin-immobilized PSMA precursor **5**.

 doi:10.20944/preprints202604.0979.v1



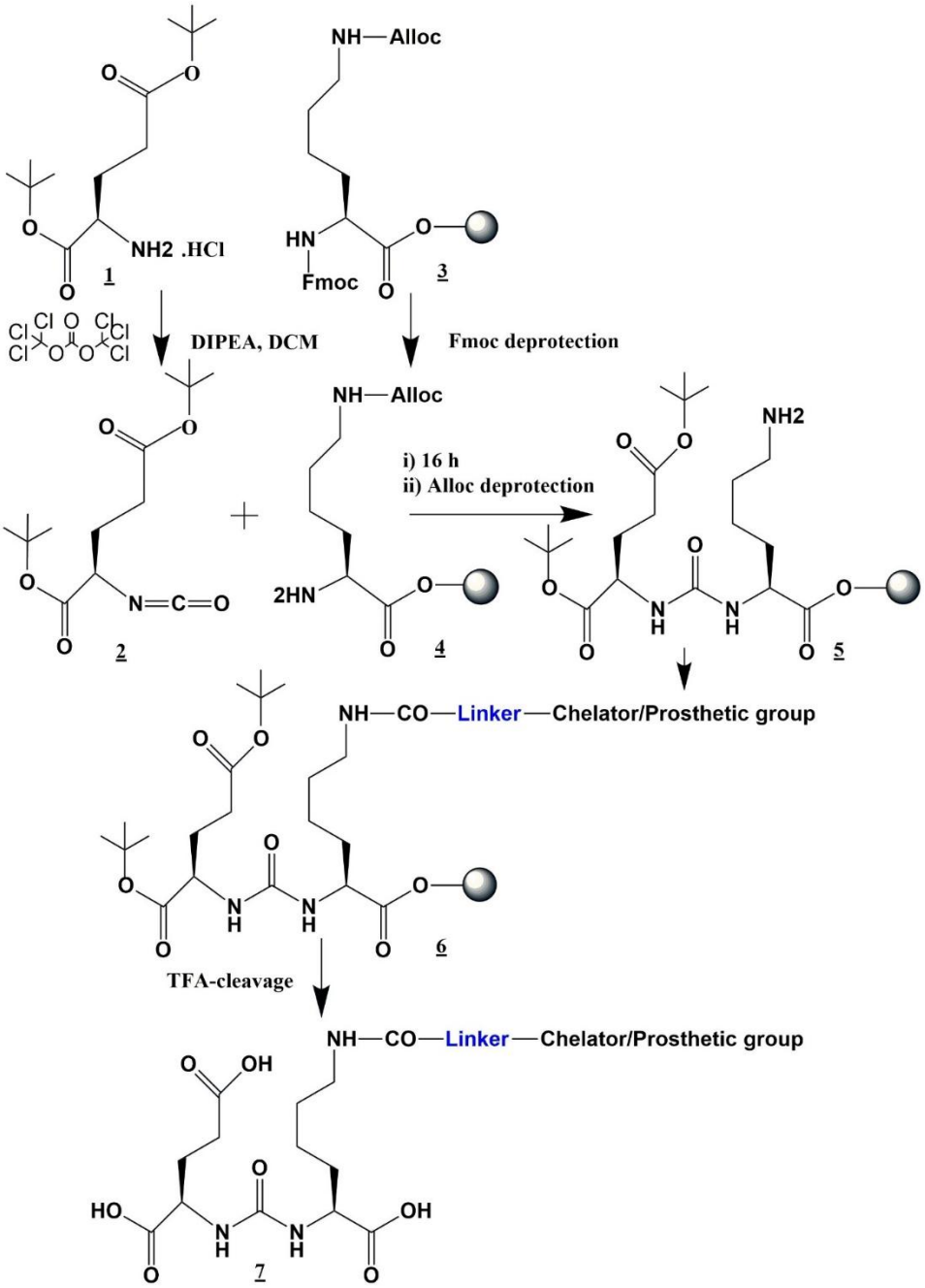


**Scheme 1.** A general method for the preparation of PSMA-targeted ligands.

The subsequent synthesis and coupling of the linker groups of the resin-immobilized peptidomimetic PSMA binding motif were performed according to the Fmoc protocol of standard solid-phase synthesis [21]. The different linker groups attached to the PSMA binding motif are described below.

Preparation of Glu-NH-CO-NH-Lys-Ahx-DiPhe-DOTA

Briefly, the attachment of the specific linker parts to the free amino group of Lys of the PSMA binding motif **5** was performed using 4 equiv. (corresponding to the resin) of Fmoc-Ahx-OH, 3.96 equiv. of HBTU (2-(1H-benzotriazol-1-yl)-1,1,3,3-tetramethyluronium hexafluorophosphate) and 8 equiv. of DIPEA. The coupling reaction was performed for 60 min at room temperature. The Fmoc group was then cleaved, and the next linker group, Fmoc-3,3-DiPhe-OH, was added identically. The conjugation of the DOTA chelator was then performed using DOTA-tris(tBu) 2.5 equiv. (corresponding to the resin), 2.5 equiv. of HBTU and 5 equiv. of DIPEA. After 4 h of reaction

 doi:10.20944/preprints202604.0979.v1



(confirmed by ninhydrin test), the PSMA peptidomimetic was cleaved from the resin by treating with a mixture consisting of 95% TFA (trifluoroacetic acid), 2.5% TIS (triisopropylsilane), and 2.5% water, to yield the desired DOTA-coupled PSMA targeting agent (Figure 4).

LC-MS (ESI): *m*/*z* calculated for $C_{49}H_{71}N_9O_{16}$, 1042.10; found: 1042.53 $[M+H]^+$ [S1].

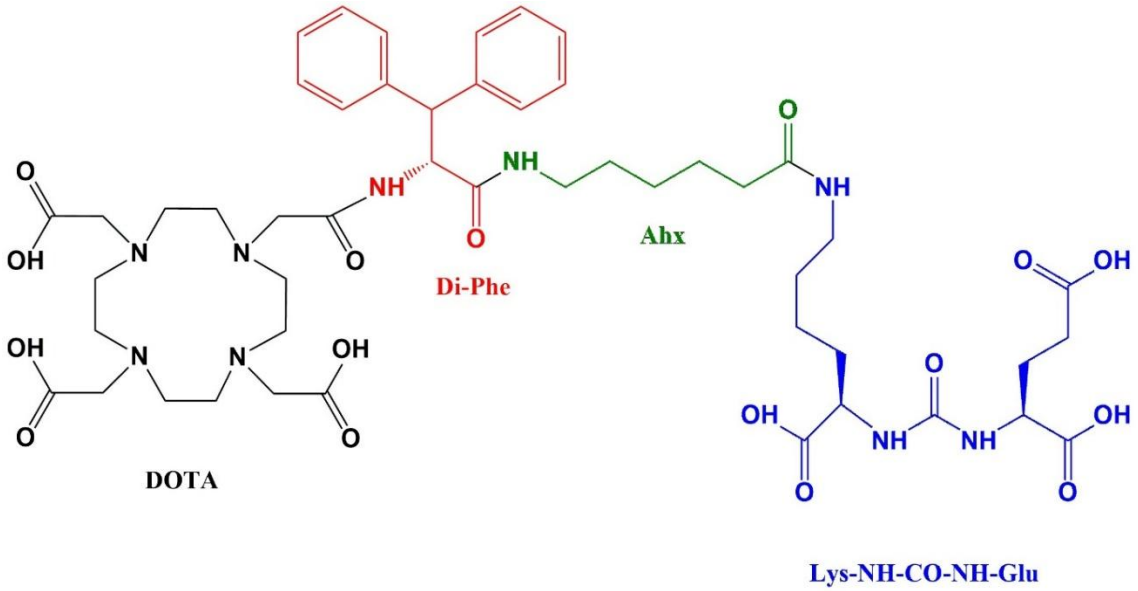


**Figure 4.** Synthetic scheme for the preparation of Glu-NH-CO-NH-Lys-Ahx-DiPhe-DOTA ligand.

Preparation of Glu-NH-CO-NH-Lys-2-NaI-Trx-Glu-Glu-Glu-DOTA

The target compound was prepared by coupling the PSMA binding motif, Glu-NH-CO-NH-Lys **5**, first with Fmoc-2-NaI-OH (Fmoc-3-(2-naphthyl)-L-alanine) using the HBTU/DIPEA protocol. Fmoc-Trx-OH (*Trans*-4-(Fmoc-aminomethyl)cyclohexanecarboxylic acid) was preactivated for 10 min in the presence of oxyma pure (Ethyl cyanohydroxyiminoacetate) (5 equiv.) and DIC (Diisopropylcarbodiimide) (5 equiv.), and allowed to react for 2 h with the resin-bound free amino group. Completion of the coupling reaction was confirmed by the Ninhydrin test. The Fmoc group was then cleaved, followed by three consecutive additions of Fmoc-Glu-OH residues, using the HBTU/DIPEA protocol. Lastly, the PSMA peptidomimetic was conjugated to DOTA-tris(tBu)ester. The cleavage from the resin is performed using a mixture of TFA:TIS:$H_2O$ as stated above (Figure 5).

LC-MS (ESI): *m*/*z* calculated for $C_{64}H_{92}N_{12}O_{25}$, 1429.45; found: 1429.63 $[M+H]^+$ [S2].

 doi:10.20944/preprints202604.0979.v1



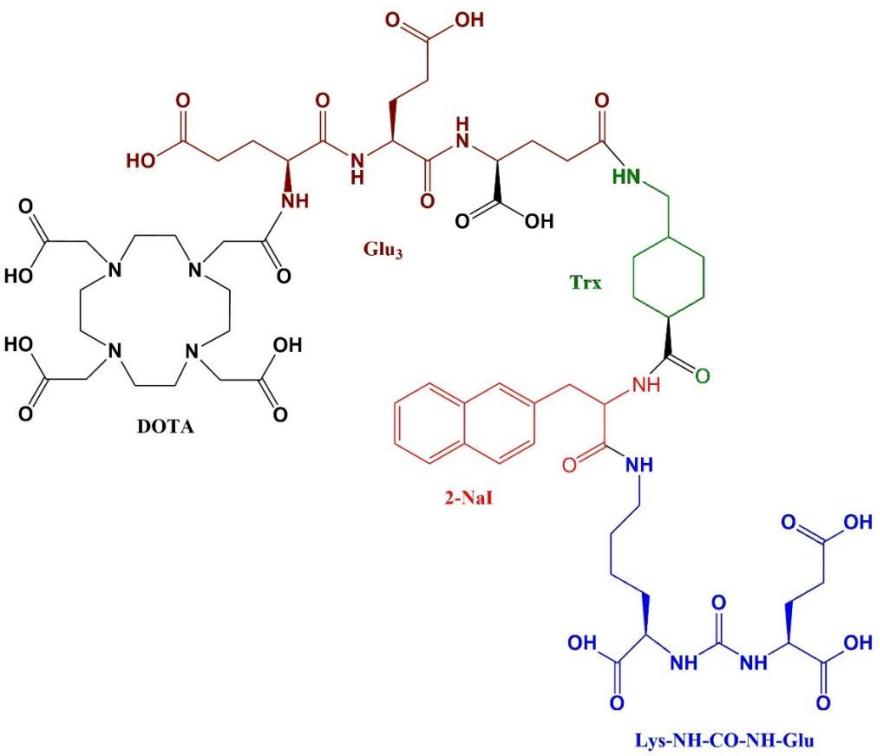


**Figure 5.** Synthetic scheme for the preparation of Glu-NH-CO-NH-Lys-2-NaI-Trx-Glu-Glu-Glu-DOTA ligand.

Preparation of Glu-NH-CO-NH-Lys-2-NaI-Trx-Aoa

The target compound was prepared by coupling the PSMA binding motif, Glu-NH-CO-NH-Lys **5**, with Fmoc-2-NaI-OH and Fmoc-Trx-OH as described above. For the introduction of an aminooxy group, Boc-Aoa-OH (5 equiv.) was preactivated for 10 min in the presence of oxyma pure (5 equiv.) and DIC (5 equiv.), and allowed to react for 2 h with the resin-bound free amino group. Completion of the coupling reaction was confirmed by the Ninhydrin test. The PSMA peptidomimetic was cleaved from the resin by treating with a mixture consisting of 95% TFA, 2.5% TIS, and 2.5% water, to yield the desired Aoa-functionalized PSMA targeting agent (Figure 6).

LC-MS (ESI): *m*/*z* calculated for $C_{35}H_{48}N_6O_{11}$, 729; found: 729.32 $[M+H]^+$ [S3].

 doi:10.20944/preprints202604.0979.v1



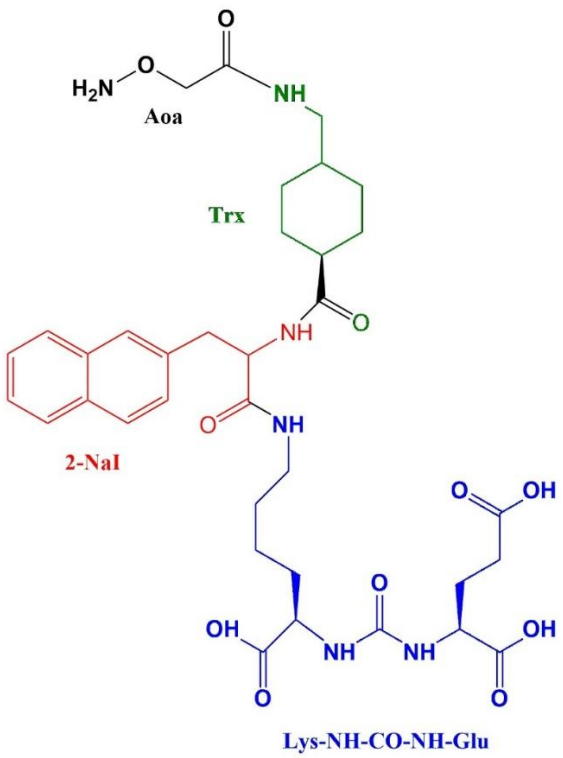


**Figure 6.** Synthetic scheme for the preparation of Glu-NH-CO-NH-Lys-2-NaI-Trx-Aoa ligand.

Preparation of Glu-NH-CO-NH-Lys-2-NaI-Trx-Glu-Glu-Glu-Aoa

The target compound was prepared as described above for the synthesis of compound Glu-NH-CO-NH-Lys-2-NaI-Trx-Glu-Glu-Glu-DOTA, except for using Aoa instead of DOTA (Figure 7).

LC-MS (ESI): *m*/*z* calculated for $C_{65}H_{90}N_{12}O_{29}$, 1503.5; found: 1504.3 $[M+H]^+$.

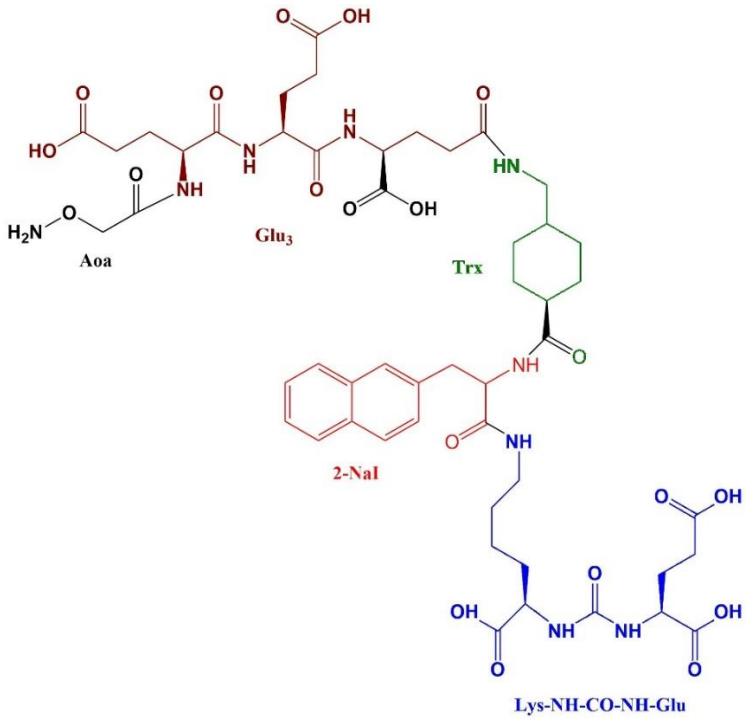


**Figure 7.** Synthetic scheme for the preparation of Glu-NH-CO-NH-Lys-2-NaI-Trx-Glu-Glu-Glu-Aoa.

Preparation of Glu-NH-CO-NH-Lys-Ahx-Aoa

 doi:10.20944/preprints202604.0979.v1



The target compound was prepared by coupling Fmoc-Ahx-OH and Boc-Aoa-OH to the PSMA binding motif, Glu-NH-CO-NH-Lys **5** (Figure 8), as described above.

LC-MS (ESI): *m*/*z* calculated for $C_{20}H_{35}N_5O_{10}$, 506; found: 506.21 $[M+H]^+$ [S4].

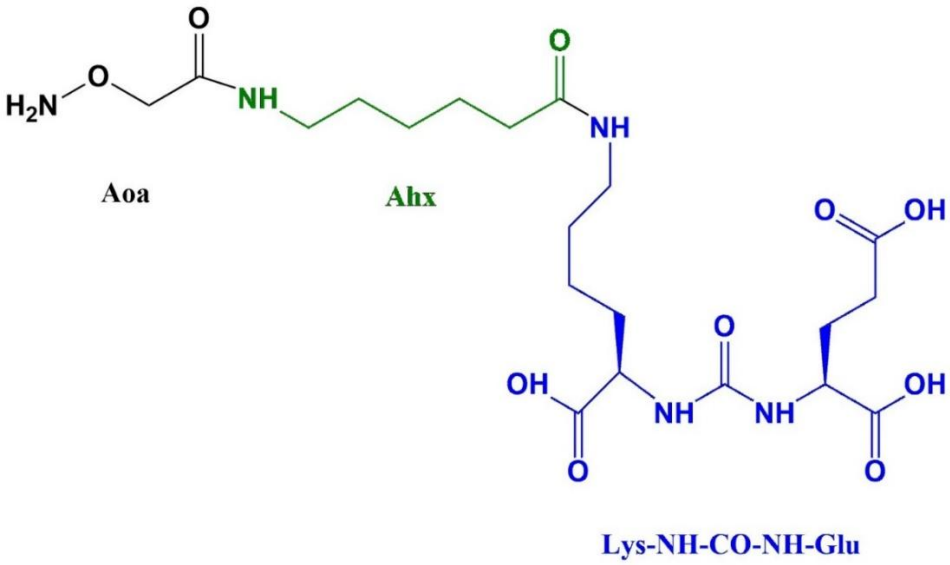


**Figure 8.** Synthetic scheme for the preparation of Glu-NH-CO-NH-Lys-Ahx-Aoa ligand.

Preparation of Glu-NH-CO-NH-Lys-4-Amb-Aoa

The target compound was prepared by coupling Fmoc-aminomethyl-benzoic acid and Boc-Aoa-OH to the PSMA binding motif, Glu-NH-CO-NH-Lys 5 (Figure 9), as described above.

LC-MS (ESI): *m*/*z* calculated for $C_{22}H_{31}N_5O_{10}$, 526; found: 527 $[M+H]^+$ [S5].

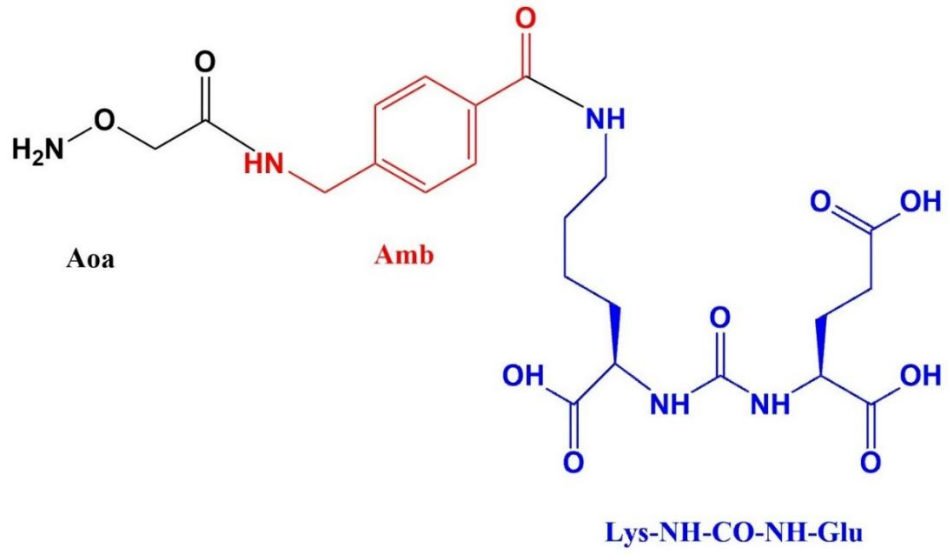


**Figure 9.** Synthetic scheme for the preparation of Glu-NH-CO-NH-Lys-4-Amb-Aoa ligand.

## 2. Synthesis of DOTA-Coupled Bis-PSMA-Binding Motif

The synthesis Scheme for the preparation of DOTA-coupled bis-PSMA ligand is presented in Figure 10. For the synthesis of the bis-PSMA ligand, the PSMA binding motif was synthesized first as described above. The free amino group of the Lys residue (Glu-NH-CO-NH-Lys-$NH_2$) was elongated by the addition of Fmoc-3,3-DiPhe-OH (4 equiv., 3.95 equiv. HBTU, 8 equiv. DIPEA, 60 min). Fmoc-Lys(ivDde)-OH was then added under identical conditions. The second PSMA binding

 doi:10.20944/preprints202604.0979.v1



motif, Glu-NH-CO-NH-Lys-COOH (prepared separately by coupling Glu-NH-CO-NH-Lys-$NH_2$ with succinic anhydride), was coupled with the free amino group of the Lys residue. The epsilon amino protection (ivDde) of the Lys residue was then cleaved to facilitate conjugation with a DOTA chelator. After washing well with DMF, DCM, and ether, the bis-PSMA conjugate was dried in a vacuum desiccator. Finally, it was cleaved from the resin by treating with a mixture of 95% TFA, 2.5% TIS, and 2.5% water, to provide the desired DOTA-coupled bis-PSMA targeting molecule.

LC-MS (ESI): *m/z* calculated for $C_{65}H_{95}N_{13}O_{25}$, 1458.5; found: 1459 $[M+H]^+$ [S6].

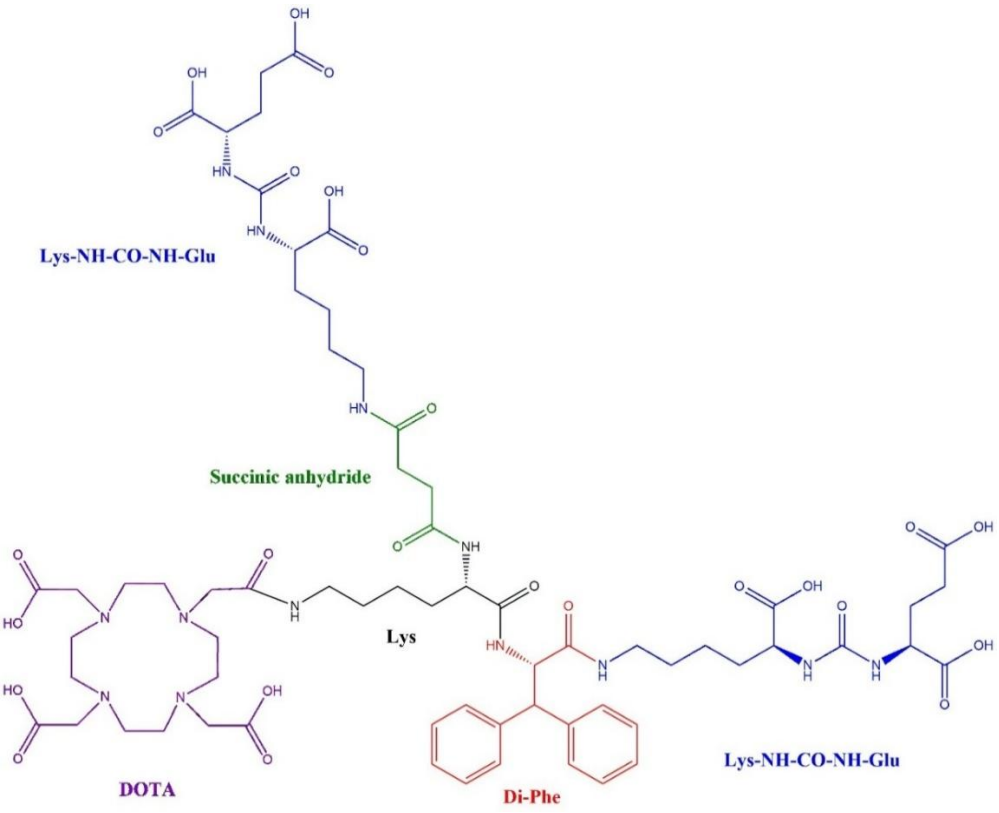


**Figure 10.** Synthetic scheme for the preparation of DOTA-coupled bis-PSMA ligand.

*Radiolabeling with $^{68}Ga$*

The radiolabeling procedure is basically as described previously [22]. Briefly, ~50 µg of DOTA-PSMA conjugate (1 mg/mL $H_2O/CH_3CN$ (1:1 v/v) solution) was mixed with 200 µL of 2.5 M sodium acetate buffer. To this, 100 µL of EtOH was added. This was followed by the addition of $[^{68}Ga]GaCl_3$ in 0.05 M HCl (111–185 MBq; 3–5 mCi, 1 mL) (eluted from $^{68}Ge$–$^{68}Ga$ generator, ITG Germany), and adjusting the pH to ~4.5. The labeling mixture was then heated for 15 min at 90 °C to enhance labeling kinetics. The reaction mixture was cooled to room temperature, and the product was purified by Sep-Pak C18, and the purity of the radiolabeled product was assessed by radio-HPLC analysis.

A non-radioactive gallium complex, $^{nat}Ga$-DOTA-bis-PSMA, was prepared by reacting DOTA-bis-PSMA (3 mg, 0.002 mmol) with Ga(III)$Cl_3$ (725 mg, 2 equiv.) dissolved in 400 µL of 0.05 M HCl. To this, 400 µL of 1.0 M sodium acetate buffer (pH 5.0) was added. The reaction mixture was heated for 60 min at 90 °C and cooled to room temperature. The product was filtered through a 0.2–µm pore syringe filter and analyzed by HPLC.

*Radiolabeling with $^{18}F$*

Approximately 300 µg of the Aoa-PSMA conjugate was dissolved in 250 µL EtOH/$H_2O$ (1:1 v/v), and to this, 200 µL of 5% AcOH in MeOH was added. After the addition of $[^{18}F]$FDG ~900 µCi (33.3 MBq) and 3 µL aniline, the labeling mixture was heated at 90 °C for 15 min in a light-shielded closed

 doi:10.20944/preprints202604.0979.v1



vial. Upon cooling, the reaction mixture was purified using a Sep-Pak C18 cartridge, and the purity of the radiolabeled product was assessed by radio-HPLC analysis [22].

*Sep-Pak C18 Purification*

The Sep-Pak C18 solid phase extraction cartridge (Waters) was preconditioned with 3 mL of ethanol and 3 mL of water. The crude product was slowly loaded onto the cartridge. The cartridge was washed with 3 mL of water to remove hydrophilic impurities. The radiolabeled product was eluted from the cartridge with 1 mL of ethanol and formulated in saline after ethanol elution. Radiochemical purity of the radiolabeled PSMA conjugates was determined by HPLC analysis.

**HPLC analysis**

HPLC analysis and purification of all seven PSMA ligands were performed on a Shimadzu HPLC system (Shimadzu, Japan) using a Phenomenex Luna C18 reversed-phase column (5 µm, 150 × 4.6 mm). For all HPLC experiments, a gradient system of 0.1% (v/v) TFA in water (solvent A) and 0.1% (v/v) TFA in $CH_3CN$ (solvent B) at a flow rate of 1.1 mL/min was used. The HPLC gradient elution was started with a solvent composition of 95% A and 5% B from 0 to 2 min, followed by a linear gradient of 95% A and 5% B to 5% A and 95% B over 25 min. The gradient remained at this position for 3 min before switching back to the initial settings of 95% A and 5% B for another 5 min. The major peak of each radiolabeled PSMA conjugate was collected, and the organic solvent was then slowly evaporated under a stream of nitrogen gas. Radiochemical purity was estimated by evaluating the radioactivity peak eluted and calculating the area under the peak (ROI). The HPLC-purified PSMA products were reconstituted in sterile saline and used for in vitro and in vivo assays.

**Octanol/water partition coefficient**

Each [$^{68}$Ga/$^{18}$F]-labeled PSMA conjugate (25 µL, ~5 µCi) was added into a glass tube containing 1 mL each of n-octanol and double-distilled water (pH = 7.4). The mixture was vortexed for 2 min and then centrifuged (5000 rpm, 5 min) to ensure the complete separation of layers. Three 100 µL aliquots from both the octanol and water layers were aspirated, and radioactivity was determined using a $\gamma$-counter. The octanol-water partition coefficient (Log $P_{o/w}$) was calculated as Log(cpm in octanol/cpm in water) [22]. The experiment was performed in triplicate.

**Stability in human plasma**

Human plasma was obtained from the institutional blood bank from healthy volunteer blood donors (with consent). The metabolic stability of the [$^{68}$Ga/$^{18}$F]-labeled PSMA conjugates was determined following a method essentially as described previously [22,23]. In summary, radiolabeled PSMA conjugate (50 µL, 100 µCi) was mixed with plasma (400 µL) and incubated in duplicate at 37 °C for up to 4 h. After incubation, the plasma proteins were precipitated using a mixture of $CH_3CN$/EtOH (1:1 v/v, 400 µL). The supernatant layer was collected by centrifugation (5000 rpm, 5 min), filtered through a 0.2-µm Millex LG syringe filter, and analyzed by radio-HPLC to determine the radiolabeled PSMA conjugate stability.

**Cell line preparation**

The cells were prepared essentially as previously described [23]. In brief, PSMA-positive LNCaP human lymph node carcinoma of the prostate cell line (American Type Culture Collection, Rockville, USA) was grown as monolayers at 37 °C in a humidified atmosphere containing RPMI-1640 culture media with 10% fetal bovine serum (FBS) in the tissue culture flasks. Twenty-four hours before conducting the tumor implantation, the media was replaced with RPMI-1640/10% FBS. The cells were grown to 80–90% confluency and harvested by trypsinization. After centrifugation, approximately 50 million cells were suspended in 2 mL PBS. For inoculation per nude mouse, approximately 5 million LNCaP cells in 200 µL sterile PBS were implanted subcutaneously into each nude mouse. Once tumor growth became sufficient (~1 cm), tumor uptake and organ biodistribution were carried out as described below.

**In vitro cell binding**

The binding of each [$^{68}$Ga/$^{18}$F]-labeled PSMA conjugate to the PSMA-positive LNCaP cell line (obtained from the ATCC, Rockville, MD, USA) was carried out essentially as described previously

 doi:10.20944/preprints202604.0979.v1



[22]. Briefly, six different concentrations of the PSMA conjugate, ranging from 1.0 to 250 nM (prepared from the serial dilutions of HPLC-purified compound), were mixed with a fixed amount of 300,000 cells (in 300 μL phosphate-buffered saline, PBS) at room temperature (21–24 °C), with slow shaking in duplicate for 60 min. The initial concentration of PSMA conjugate was determined following a known HPLC technique with simultaneous detection by UV absorbance [22]. Incubation was terminated by dilution with cold PBS (200 μL), followed by centrifugation. The supernatant was collected, and cell pellets were rapidly washed with cold PBS to remove any unbound radioestradiol. Radioactivity in the cell pellet (total bound) and the supernatant (unbound) was measured using a γ-counter. Nonspecific binding was determined in the presence of approximately a 200-fold molar excess of unlabeled PSMA compound. Specific binding is calculated by subtracting the non-specifically bound radioactivity from that of the total binding. The dissociation constant ($K_d$) is calculated using a plot of cell-bound activity versus the concentrations of the radioligand using the GraphPad Prism software version 6 (GraphPad Software Inc., San Diego, CA, USA). The experiment was performed in triplicate.

**Dose preparation**

For in vivo biodistribution studies, doses were prepared by dissolving the HPLC-purified [$^{68}$Ga/$^{18}$F]-labeled PSMA conjugates in sterile saline to a concentration of ~100 μCi/mL. For PET animal imaging studies, doses were prepared by dissolving the [$^{68}$Ga/$^{18}$F]-labeled PSMA conjugates in saline to ~1.5 mCi/mL. For the receptor-blocking experiment, each PSMA conjugate was dissolved in a dose solution of ~2 mg/mL. The resulting dose solution was filtered with a 0.2-μm Millex LG syringe filter before being injected into animals. Each animal was injected with ~100 μL of the dose solution.

**In vivo tumor uptake study**

Approval from the Institutional Animal Care and Use Committee was obtained for the animal protocol used. In addition, strict international regulations govern the safe and proper use of laboratory animals employed during animal experiments. Mice used for this research were housed under controlled conditions of 12 h of light/dark cycles, temperature (20–24 °C), humidity (40–60%), and free access to regular commercial mouse feed and water. In vivo tumor uptake was conducted following the method reported previously [22,23]. In short, tumor uptake and tissue biodistribution studies were carried out in male nude mice ($n$ = 3–5 per time point, body mass 20–25 g) at 45 min and 2.5 h post-injection. Each animal was administered with the HPLC-purified [$^{68}$Ga]- or [$^{18}$F]-labeled PSMA conjugate (100 μL, 20–25 μCi) via lateral tail vein injection. At the specified time points, the PSMA-positive xenografted nude mice were sacrificed by cervical dislocation. A fraction of the blood (~100 μL) was collected from cardiac puncture. Urine was also collected and measured with the bladder contents. The tumor was dissected, and major organs, such as the lungs, pancreas, stomach, liver, heart, kidneys, and intestines, were isolated, weighed, and measured for radioactivity. The percent of the injected dose or injected activity per gram (% ID/g) in the tumors and body organs was determined by using a custom-designed Quattro Pro X9 spreadsheet (Corel Corporation, USA). The uptake values of the PSMA conjugate are expressed as the % ID/g of tissue/organ. The radioactivity in the urine with bladder contents is shown as the % ID. To calculate the injected activity, a standard (20-fold dilution of injected activity) was prepared and counted together with animal tissue samples.

For the PSMA receptor blocking study, an additional group of mice was injected with the [$^{68}$Ga]Ga-DOTA-PSMA conjugate premixed with a 200-fold molar excess of unlabeled PSMA compound (50 μL, 100 μCi). In vivo biodistribution and blocking studies were performed at 2.5 h p.i. as stated before.

**Small animal PET imaging**

Micro PET imaging was conducted as described previously with some modifications [22]. To find out the tumor-targeting potential of the [$^{68}$Ga]-DOTA-Bis-PSMA ligand, (100 μL, ~100 μCi) of the radiotracer was administered through the tail vein injection into a nude mouse carrying LNCaP tumor xenografts. After 45 min and 2.5 h p.i., the mouse was sedated and placed in the camera bed, and a total of 15-min static images, with a 15-min frame, were acquired in the prone position using a mini-PET camera (Bioemtech, Athens, Greece). The PET camera is equipped with a pixelated BGO

 doi:10.20944/preprints202604.0979.v1



(bismuth germanate) scintillator and four arrays of compact position-sensitive photomultiplier tubes with a field of view of 48 mm x 98 mm and an intrinsic spatial resolution of ~1.5 mm. The manufacturer preinstalled concurrent image reconstruction software Visual Eyes, which was used to convert the acquired frames into 2D image visualization. Images were then generated using ImageJ software (National Institute of Health, USA). Following imaging, animals were dissected, and quantitative biodistribution was performed to validate the findings of the PET imaging.

**Statistical analysis**

Experimental data are represented as mean ± S.D. where appropriate. For data evaluation, mean values were compared using the Student's *t*-test (GraphPad Software, San Diego, CA), and a probability value ($P$) <0.05 was considered statistically significant.

## 3. Results

*Synthesis*

Both DOTA-coupled and aminooxy-functionalized PSMA conjugates (Scheme 1) were successfully synthesized on a wang resin following standard peptide chemistry protocols. The "Glu-NH-CO-NH-Lys" pharmacophore remains the main core of the structure of all seven newly synthesized PSMA analogs. Starting from the formation of the glutamate moiety, several linker groups, such as DiPhe, Glu, Ahx, and Amb, were attached to the PSMA binding motif using Fmoc-based solid-phase peptide synthesis. Lastly, DOTA or Aoa were introduced to facilitate radiolabeling with $^{68}$Ga and $^{18}$F, respectively. All PSMA ligands were synthesized with higher than 40% overall yield.

The bispecific PSMA ligand was synthesized by starting with the isocyanate of the glutamyl moiety using standard peptide synthesis protocols. Fmoc-DiPhe-OH was used as a linker group. In parallel, the second PSMA with a free COOH group was prepared and coupled to the PSMA peptidomimetic via the free amine group of the Lys residue. It was then conjugated to DOTA to yield the desired DOTA-bis-PSMA targeting molecule in a good yield of 41%. The structural identities of all the synthesized PSMA peptidomimetics were confirmed by ESI mass spectrometry detection.

**Radiolabeling with $^{68}$Ga and $^{18}$F**

DOTA-coupled PSMA conjugates were radiolabeled efficiently with $^{68}$Ga simply by dissolving the PSMA conjugate in NaOAc buffer, followed by the addition of [$^{68}$Ga]$GaCl_3$ radioactivity and heating the reaction mixture to accelerate the radiolabeling kinetics. These facile procedures provide reproducible and efficient radiolabeling (~90%) of all three PSMA conjugates via DOTA chelator with $^{68}$Ga radionuclide, with molar radioactivity in the range of 30-300 mCi/mg. The radio-HPLC analyses revealed that the [$^{68}$Ga]-labeled PSMA conjugates formed mainly one radioactive species, with retention time between 12 and 13 min. Under the same HPLC conditions, free $^{68}$Ga was eluted at around 3–4 min. For radiolabeling with $^{18}$F, [$^{18}$F]FDG is used as a prosthetic group for radiolabeling PSMA conjugate via the oxime formation of [$^{18}$F]FDG-Aoa-PSMA conjugates in the presence of a small amount of aniline (3 μL) as a nucleophilic catalyst, under mild acidic aqueous conditions. This procedure provides reproducible and good radiochemical purity of greater than 80% (range, between 81% and 93%) of all the Aoa-PSMA conjugates evaluated in this study, with molar radioactivity in the range of 25-250 mCi/mg. The radio-HPLC analyses showed that the [$^{18}$F]FDG-PSMA conjugates formed mainly one radioactive product, with a retention time between 12 and 13 min. The free [$^{18}$F]FDG peak was eluted on the HPLC at around 3 min. Both [$^{68}$Ga/$^{18}$F]-labeled PSMA conjugates have shown stability for at least up to 4 h at room temperature as revealed by radio-HPLC analysis. Representative HPLC chromatograms are presented in Figure 11. Furthermore, the identification of the [$^{68}$Ga]Ga-DOTA bis-PSMA complex was confirmed by co-injecting the nonradioactive $^{nat}$Ga-DOTA-bis-PSMA ligand, as it displayed a nearly similar retention time UV profile to that of [$^{68}$Ga]Ga-DOTA bis-PSMA conjugate under the same HPLC conditions (Figure 11).

 doi:10.20944/preprints202604.0979.v1



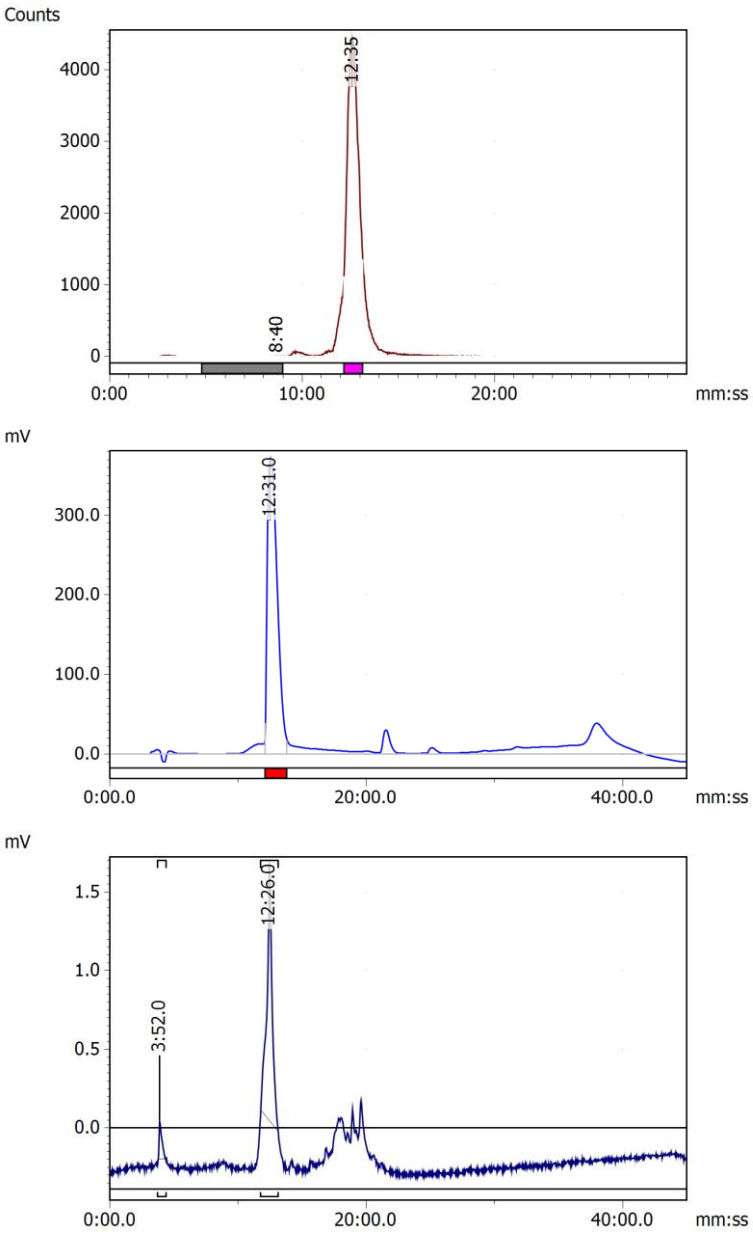


**Figure 11.** Representative HPLC chromatograms of the [$^{68}$Ga]-DOTA-bis-PSMA ligand at 45 min post-labeling (*upper*); and UV chromatogram of the DOTA-bis-PSMA ligand (*middle*); the reference $^{nat}$Ga-DOTA-bis-PSMA ligand at UV 220 nm for the identity confirmation (*lower*).

**Table 1.** Characteristics of the [$^{68}$Ga/$^{18}$F]-labeled PSMA ligands evaluated in this study. Bold letter represents the compound named in this study.

| Compound | Molecular weight | HPLC retention time (min) | Log *P* | Binding affinity (nM) |
|---|---|---|---|---|
| [$^{68}$Ga]-DOTA-PSMA 617 **[$^{68}$Ga]-PSMA-617** | 1042.14 | 13.15 | -2.63±0.12 | 25.72 ± 4.84 |
| [$^{68}$Ga]-DOTA-Di-Phe-Lys-CO-Glu-OH **[$^{68}$Ga]-Di-Phe** | 1042.15 | 13.06 | -2.86±0.13 | 66.43 ± 12.35 |

 doi:10.20944/preprints202604.0979.v1



| | | | | |
|---|---|---|---|---|
| [$^{68}$Ga]-DOTA-Glu$_3$-Lys-CO-Glu-OH **[$^{68}$Ga]-Glu3** | 1429.4 | 12.45 | -3.09±0.11 | 59.12 ± 10.13 |
| [$^{68}$Ga]-DOTA-Bis-PSMA-(Lys-CO-Glu)$_2$ **[$^{68}$Ga]-Bis-PSMA** | 1458.5 | 12.35 | -3.18±0.15 | 39.92 ± 9.89 |
| [$^{18}$F]-Aoa-2-NaI-Trx-Lys-CO-Glu-OH PSMA-617 **[$^{18}$F]-PSMA-617** | 729 | 13.0 | -1.51±0.11 | 40.09 ± 8.76 |
| [$^{18}$F]-Aoa-Glu3 Lys-CO-Glu-OH **[$^{18}$F]-Glu3** | 1503.5 | 12.39 | -2.40±0.13 | 72 ± 14.50 |
| [$^{18}$F]-Aoa-Ahx Lys-CO-Glu-OH **[$^{18}$F]-Ahx** | 506 | 13.3 | -1.11±0.10 | 94.10 ± 13.78 |
| [$^{18}$F]-Aoa-Amb-Lys-CO-Glu-OH **[$^{18}$F]-Amb** | 526 | 12.49 | -2.16±0.12 | 93.0 ± 15.04 |

**Partition coefficient determination**

The lipophilicities of all the [$^{68}$Ga/$^{18}$F]-labeled PSMA ligands were determined by measuring their radioactivity distribution ratios between *n*-octanol and water layers with pH 7.4. In all cases, negative values of the partition coefficient (log *P)* were observed, indicating the preference of all the tested PSMA ligands towards the water phase. The obtained log *P* values ranged from -1.11 to -3.18, indicating variable degrees of hydrophilicity of the PSMA conjugates under evaluation. The reference compound [$^{68}$Ga]Ga-PSMA-617 exhibited a low hydrophilicity, with a log *P* value of -2.63 ± 0.12. The highest hydrophilicity value of -3.18 ± 0.15 was observed for the Bis-PSMA compound. Also, the PSMA compound containing three glutamic acid residues displayed a high hydrophilicity value of -3.09 ± 0.11, while the PSMA conjugate with aminohexanoic acid linker displayed the lowest hydrophilicity (-1.11 ± 0.10) among the tested PSMA compounds. The partition coefficient values of all tested radiolabeled PSMA compounds are presented in Table 1.

**In Vitro Metabolic Stability in Human Plasma**

The extent of proteolytic degradation of the [$^{68}$Ga/$^{18}$F]-labeled PSMA conjugates was determined in human plasma and assessed by HPLC. The metabolic stability ranged between 70% and 83% for [$^{68}$Ga]-labeled PSMA conjugates, whereas for the [$^{18}$F]-labeled PSMA conjugates, the range was between 72% and 80% after 2.5 h of incubation. No major peaks of any radiometabolites were observed except for the minor peaks between 3 and 4 min., indicating the limited release of the free amount of $^{68}$Ga and $^{18}$F (up to 30%). The data emphasized the high in vitro plasma stability of the [$^{68}$Ga/$^{18}$F]-labeled PSMA conjugates, with low enzymatic breakdown by plasma proteases (Figure 12).

 doi:10.20944/preprints202604.0979.v1



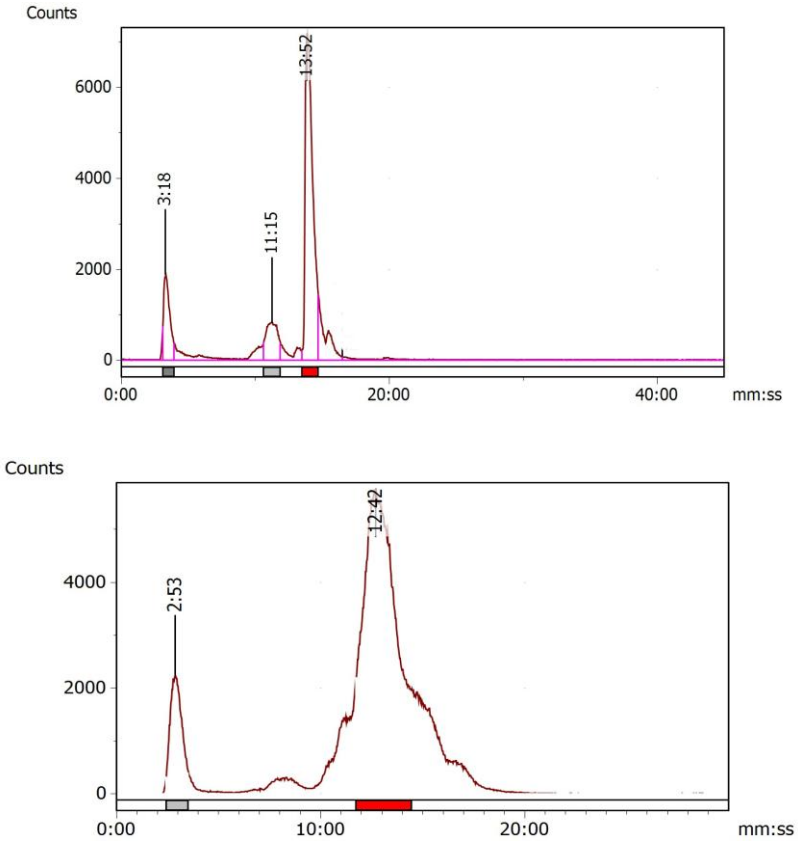


**Figure 12.** Representative radio-HPLC chromatograms of the [$^{68}$Ga]-DOTA-Bis-PSMA ligand after 2.5 h incubation with human plasma (upper), and the analysis of the urine sample collected at 2.5 h post-injection of [$^{68}$Ga]-DOTA-Bis-PSMA ligand.

**In Vitro Tumor Cell Binding**

Human prostate cancer cell line, namely LNCaP, with high PSMA expression, was used to investigate the binding potential of [$^{68}$Ga/$^{18}$F]-labeled PSMA conjugates. The binding affinity ($K_d$) was determined using the saturation binding by fitting the data with nonlinear regression using the Graph-Pad Prism program. All tested PSMA compounds exhibited a specific affinity to PSMA with a low to moderate nanomolar binding affinities, using the LNCaP cells ($K_d$ values ranging from 39.92 ± 9.89 nM to 94.10 ± 13.78 nM; Table 1). [$^{68}$Ga]Ga-PSMA-617 was also evaluated as a reference standard (25.72 ± 4.84 nM). [$^{68}$Ga]Ga-DOTA-PSMA conjugates showed a good binding affinity in the range of 59.12 to 66.43 nM, while comparable or in some cases slightly lower binding affinity values were obtained for the [$^{18}$F]FDG-PSMA conjugates, which varied from 40.09 to 94.10 nM. The binding with the LNCaP cells was significantly inhibited in the presence of a 200-fold molar excess of unlabeled PSMA molecule, demonstrating the PSMA receptor specificity of the [$^{68}$Ga/$^{18}$F]-labeled PSMA conjugates under investigation. The introduction of glutamate or DiPhe moieties in the PSMA core resulted in a decrease of binding affinity when compared with the reference compound [$^{68}$Ga]Ga-DOTA-PSMA-617. The bis-PSMA compound exhibited about 1.7 times better binding affinity (39.92 ± 9.89) than the corresponding monomer compound (66.43 ± 12.35 nM), suggesting a good impact of bis-PSMA on the binding characteristics. An example of binding affinity measurement by nonlinear regression using the Graph-Pad Prism program is presented in Figure 13.

 doi:10.20944/preprints202604.0979.v1



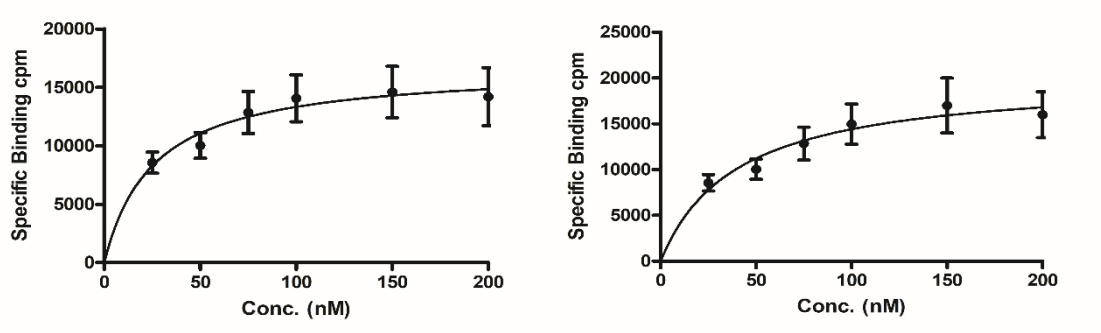


**Figure 13.** In vitro saturation cell binding of [$^{68}$Ga]-DOTA-PSMA-617 (left) and [$^{68}$Ga]-DOTA-Bis-PSMA ligand (right), with PSMA-positive LNCaP cancer cell line. [$^{68}$Ga]-DOTA-PSMA-617 displayed a binding affinity of 25.72 nM, whereas [$^{68}$Ga]-DOTA-Bis-PSMA showed the cell binding affinity, with the $K_d$ value of 39.92 nM ($n$=3).

**In Vivo Tumor Targeting and Biodistribution Studies**

The in vivo biodistribution and tumor targeting potential of the [$^{68}$Ga/$^{18}$F]-labeled PSMA conjugates were investigated in male nude mice carrying PSMA-positive LNCaP xenografts at 45 min and 2.5 h post intravenous injection in order to determine their ability to target human prostate cancer in vivo. The biodistribution data are presented in Figures 14 and 15. In general, all the [$^{68}$Ga/$^{18}$F]-labeled PSMA conjugates tested showed a rapid clearance from the blood, as less than 1% ID/g of radioactivity was present in the blood after 2.5 h p.i.

The highest uptake value of 3.51% ± 0.90% ID/g in the tumors was observed for $^{68}$Ga-DOTA-bis-PSMA ligand as early as 45 min p.i., which was reduced to 2.05% ± 0.63% ID/g at 2.5 h p.i. The same leading bis-PSMA ligand also exhibited good binding affinity to the LNCaP cells. The Aoa-functionalized PSMA 617 also exhibited a good tumor uptake of 3.10 ± 0.72% ID/g, which is fairly lower than the corresponding [$^{68}$Ga]Ga-DOTA-PSMA 617 (4.03 ± 0.82% ID/g). The data suggest that the introduction of the negatively-charged Glu residues only minimally improved the tumor-targeting properties of the PSMA compound, as 2.97 ± 0.64% ID/g was found in the tumors at 45 min p.i. In general, the [$^{68}$Ga/$^{18}$F]-labeled PSMA conjugates under investigation displayed moderate accumulation in the tumors, with the values varying from 2.02% ± 0.39% to 3.51% ± 0.91% ID/g at 45 min and from 1.04% ± 0.24% to 2.05% ± 0.66% ID/g at 2.5 h p.i. Despite this, all radiolabeled PSMA conjugates showed a higher accumulation of radioactivity in the tumors than in the blood and muscle, resulting in good tumor-to-blood and tumor-to-muscle ratios (Figure 16). The accumulation in receptor-positive organs, such as the intestines, spleen, and stomach, was low to moderate (except for the kidneys) and was below 4% ID/g for all the radiolabeled PSMA conjugates.

The [$^{68}$Ga/$^{18}$F]-labeled PSMA conjugates having different partition coefficient values displayed variable degrees of uptake in the liver, with the amount retained ranging from 0.51% ± 0.19% to 2.03% ± 0.42% ID/g at 1 h and from 0.39% ± 0.13% to 0.82% ± 0.29% ID/g at 2.5 h p.i. The most hydrophilic compound (log $P$ = -3.18) was found to be the [$^{68}$Ga]-DOTA-Bis-PSMA, which showed a liver uptake of 0.74 ± 0.20% ID/g and 0.50 ± 0.12% ID/g at 45 min and 2.5 h p.i., respectively. The radioactivity present in the liver for the reference compound [$^{68}$Ga]Ga-DOTA-PSMA 617 was 0.50 ± 0.11% ID/g and 0.39 ± 0.10% ID/g at 45 min and 2.5 h p.i., respectively.

Accumulation in the kidneys ranged from 2.02% ± 0.53% ID/g to 6.11% ± 1.13% ID/g at 45 min and from 1.03% ± 0.47% to 3.90% ± 1.0% ID/g at 2.5 h p.i, demonstrating the variable uptake and retention of these PSMA complexes by the kidneys. The [$^{18}$F]-labeled PSMA conjugate, comprising Ahx linker, showed the highest uptake in the kidneys (6.11% ID/g, 45 min p.i.), whereas the [$^{18}$F]-labeled PSMA ligand, with a benzene moiety containing Amb linker, exhibited the lowest kidney uptake (2.02% ID/g, 45 min p.i.), among the tested compounds. Interestingly, when compared with the reference [$^{68}$Ga]Ga-DOTA-PSMA-617, all the compounds tested in this study showed relatively lower kidney uptake and retention at both the studied time points. High kidney uptake/retention is not desirable for diagnostic imaging and, in particular, for therapy because of potential nephrotoxicity [25]. The main route of excretion of the [$^{68}$Ga/$^{18}$F]-labeled PSMA conjugates in mice

 doi:10.20944/preprints202604.0979.v1



was through the renal/urinary system. The amount of the radioactivity excreted into the urine was up to 54% ID, while the clearance of the radiolabeled conjugates through the hepatobiliary system (liver + intestines) was insignificant (below 6% ID). In general, no marked difference, except for the kidneys' uptake and retention, was observed between the biological and tumor uptake behavior of the PSMA conjugates, radiolabeled either with [$^{68}$Ga] or [$^{18}$F], highlighting the low impact of the radionuclides on the biological and tumor targeting characteristics of the PSMA conjugates.

A low to moderate uptake of radioactivity (below 4% ID/g) was observed in the stomach, lungs, spleen, and intestine (with contents), at all times, suggesting the favorable pharmacokinetics of these PSMA ligands. Because of the low hepatobiliary (liver + intestines) uptake, all the PSMA displayed good excretion via the renal system. Radioactivity concentrated in the muscle/bone was found to be low both at 45 min and 2.5 h p.i. (below 0.30% ID/g).

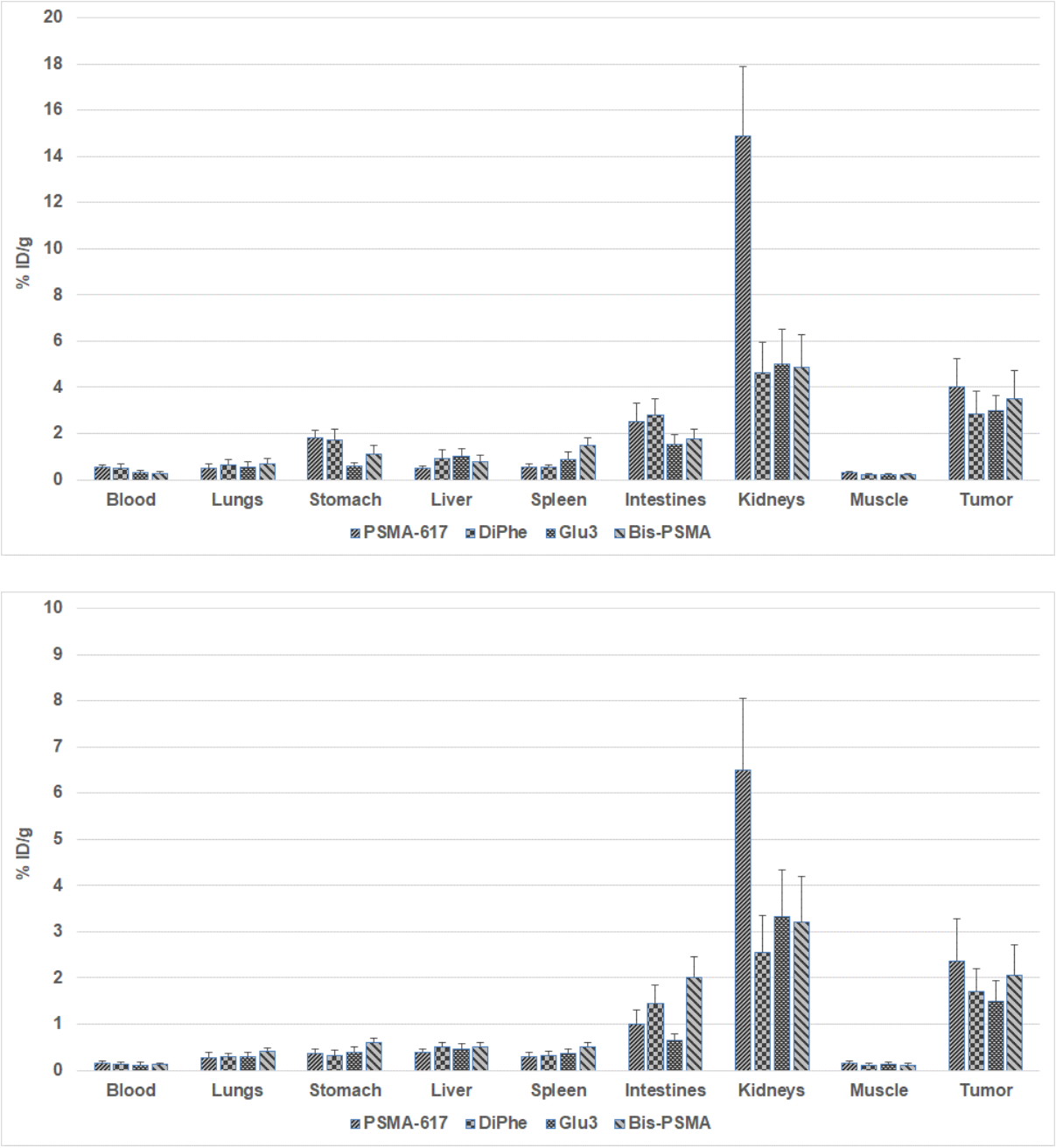


**Figure 14.** In vivo uptake values of [$^{68}$Ga]-DOTA PSMA ligands in selected organs of male nude mice, with LNCaP tumor xenografts at 45 min (upper) and 2.5 h (lower) post-injection. All values are expressed as %ID/g. Data represent mean values ± SD from at least 3 determinations.

 doi:10.20944/preprints202604.0979.v1



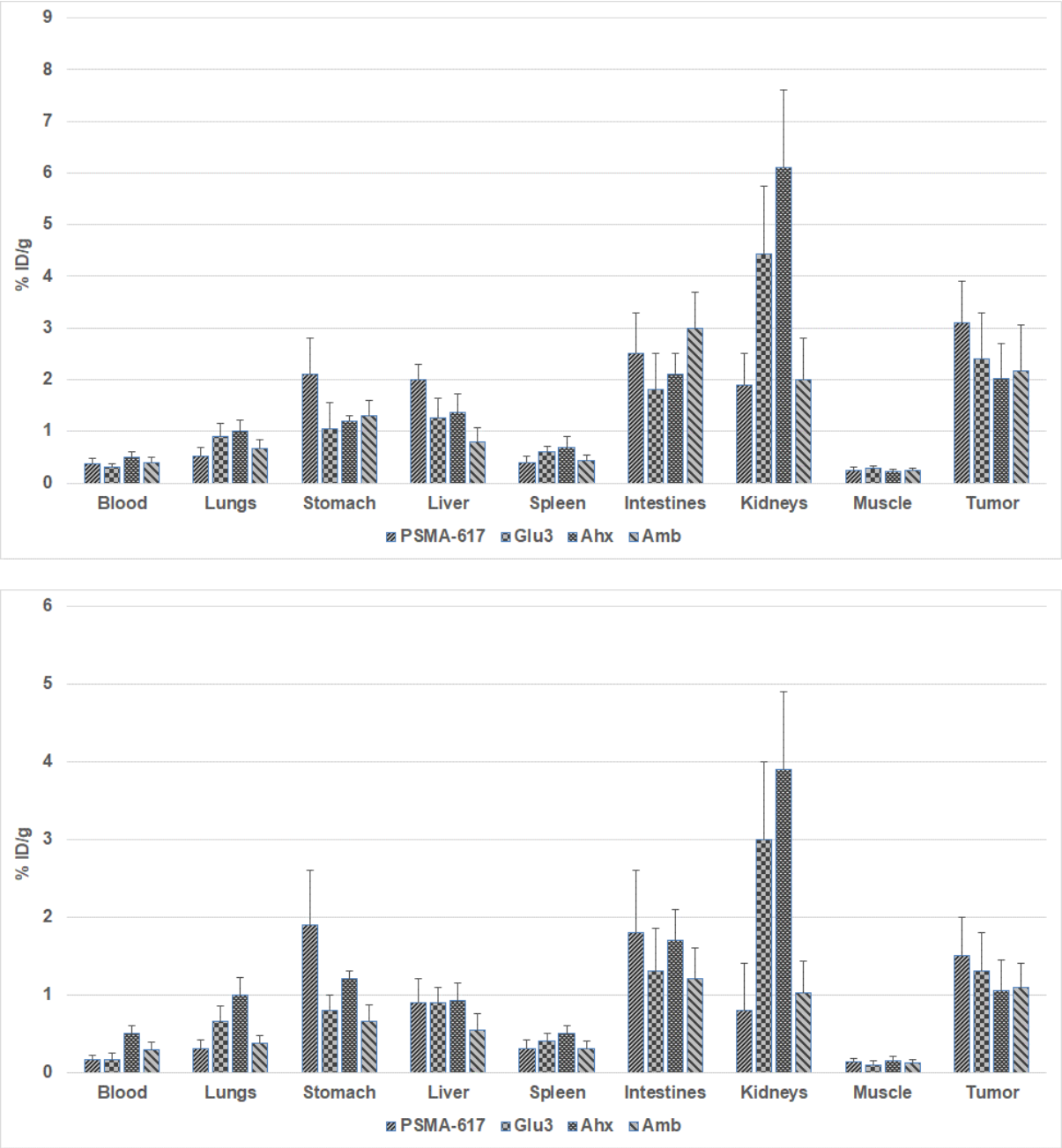


**Figure 15.** In vivo uptake values of [$^{18}$F]-labeled PSMA ligands in selected organs of male nude mice, with LNCaP tumor xenografts at 45 min (upper) and 2.5 h (lower) post-injection. All values are expressed as %ID/g. Data represent mean values ± SD from at least 3 determinations.

Tumor-to-nontumor ratios were also calculated and are depicted in Figure 16. A trend of improved tumor-to-blood and tumor-to-muscle uptake ratios over time was observed for most of these PSMA compounds, possibly due to the rapid clearance from the blood and other organs and tissues. The tumor-to-blood ratios for the [$^{68}$Ga/$^{18}$F]-labeled PSMA ligands ranged from 4.90 to 13.65 at 45 min and from 4.95 to 16.92 at 2.5 h p.i., whereas tumor-to-muscle ratios ranged from 7.43 to 17.85 at 45 min and from 8.08 to 20.30 at 2.5 h p.i., indicating the possible potential of these PSMA conjugates for targeting prostate cancer in vivo.

 doi:10.20944/preprints202604.0979.v1



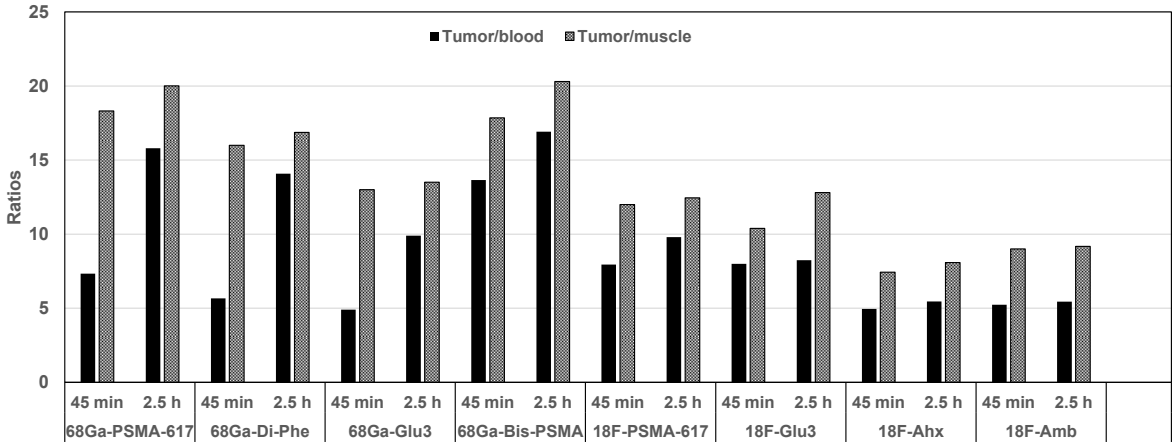


**Figure 16.** Tumor-to-blood and tumor-to-muscle uptake ratios for the [$^{68}$Ga/$^{18}$F]-labeled PSMA conjugates in nude mice bearing LNCaP tumor xenografts at 45 min and 2.5 h post-injection.

Radio-HPLC analysis of the urine samples collected at 2.5 h p.i. of the radiolabeled PSMA compounds indicated that most of the radioactivity was still associated with the radiolabeled PSMA conjugates, revealing low in vivo degradation of these radiolabeled PSMA conjugates. It was found that both [$^{68}$Ga] and [$^{18}$F]-labeled PSMA conjugates have shown nearly similar in vivo stability, highlighting the low impact of the radionuclide on the complex stability.

An in vivo receptor-blocking study was also carried out, where a 0.2 mg dose of the PSMA molecule per mouse was co-injected for in vivo saturation of receptors. It was found that the blocking dose reduced the uptake in the tumors, ranging from 51% to 67%, advocating the in vivo receptor specificity of these PSMA conjugates for receptor-positive tumors. Also, a variable influence of the PSMA blocking dose was observed in the major organs, such as the stomach, spleen, intestines, and kidneys, probably related to the variable levels of PSMA receptor-expression by some of these organs [2–4].

## Small Animal PET Imaging

The tumor imaging ability of the bis-PSMA ligand was further examined in male nude mice with subcutaneous PSMA-expressing tumor xenografts at 45 min and 2.5 h p.i. Even though a significant accumulation of radioactivity was seen in the kidneys together with the urinary bladder, the implanted LNCaP tumors are reasonably detectable in the PET image (Figure 17), possibly due to the efficient clearance of the radiolabeled PSMA conjugate from the adjacent organs and tissues. A high urinary bladder radioactivity indicates the major route of excretion. Overall, PET imaging suggests the potential of [$^{68}$Ga]-DOTA-bis-PSMA conjugate to image PSMA-positive LNCaP prostate carcinomas. Following the imaging study, quantifiable tissue biodistribution was performed to confirm the findings of the PET imaging, and found to agree with the findings of the PET imaging.

 doi:10.20944/preprints202604.0979.v1



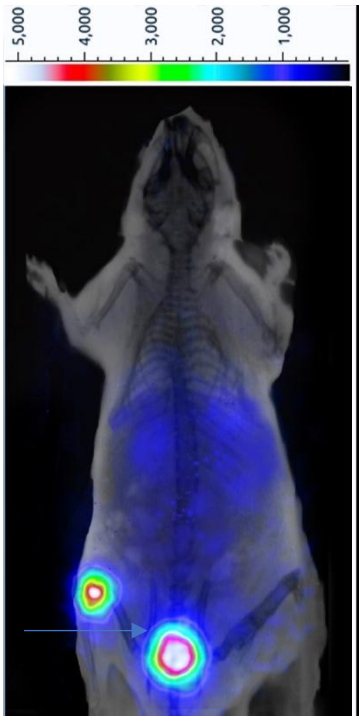


**Figure 17.** Micro-PET camera image of a male nude mouse model, with PSMA-positive LNCaP tumor xenograft at 45 min post-intravenous tail injection of approximately 100 μCi of [$^{68}$Ga]-DOTA-Bis-PSMA ligand. High urinary bladder activity can be seen in the image. The arrow indicates the tumor location.

## 4. Discussion

As PCa continues to be the most frequently diagnosed cancer and one of the main causes for cancer-related deaths amongst men, more focus on the development of new or improved radiopharmaceuticals for PCa is warranted [1–4]. Radionuclide molecular imaging using PET allows highly precise and sensitive detection of microscale tumor lesions. The use of radioligands with the ability to bind to PCa-specific biomarkers makes molecular imaging a promising approach for both diagnosis and staging, as well as monitoring treatment outcomes. In almost all types of prostate cancer, the majority of primary and metastatic lesions show PSMA expression [1,4,5]. Radioligands binding to PSMA receptors have played a positive role in the clinical diagnosis and treatment of PCa. However, PET-based diagnosis of PCa still faces challenges due to suboptimal pharmacokinetics, resulting in insufficient tumor retention and consequently reduced sensitivity in detecting metastatic lesions. To address these issues, various chemical optimization approaches have been applied, including modification of the linker between the chelator site and the Glu-urea-Lys pharmacophore. It has been shown that aromatic amino acids, as well as charged amino acid-based linkers, typically improve the pharmacokinetics and tumor-targeting behavior of PSMA molecules [9,10,14,15]. Furthermore, we designed and constructed a bis-PSMA ligand, containing two PSMA targeting motifs (Glu-urea-Lys) in a single molecule, along with the metal-chelating moiety DOTA for radiolabeling, to determine its effectiveness over the corresponding monovalent PSMA counterpart. The goal of this study was to investigate the effectiveness of the PSMA mono and bis conjugates radiolabeled either with [$^{68}$Ga] and [$^{18}$F] for targeting PSMA receptors overexpressed on PCa. Here, we report the chemical synthesis, radiolabeling with [$^{68}$Ga] and [$^{18}$F], in vitro and in vivo evaluations to examine the newly developed PSMA molecules to determine their ability to target LNCaP prostate cancer cell lines in preclinical settings.

The synthesis of PSMA conjugates was performed essentially according to standard peptide chemistry protocols [21]. Using the Lys-CO-Glu-OH pharmacophore as a basic core structure, our interest in attaching different linker groups triggered us to synthesize 7 different PSMA ligands, with the general structure of Glu-urea-Lys-X-DOTA/Aoa, where X was the position of substitution and/or

 doi:10.20944/preprints202604.0979.v1



addition of linker groups. To determine the effect of the nature of the chelate and the length and composition of the linker on binding affinity, we focused in this study, towards the developing of PSMA analogs in which amino acids, such as DiPhe, Glu, Ahx or Amb are linked to Glu-urea-Lys binding core to improve binding and tumor targeting characteristics as well as to reduce kidney uptake/retention of the resultant PSMA analogs. These diverse linkers are selected because of their ease of synthesis and conjugation by solid-phase synthesis to the PSMA binding motif. The effect of the nature of the chelate, as well as the length and composition of the linker, on binding affinity and biological activity is evaluated herein. In addition to the monomers, we also conveniently synthesized a bis-PSMA ligand containing the two PSMA binding motifs within one construct, and compared its binding and tumor-targeting potential with the corresponding monomers.

To allow radiolabeling of PSMA compounds with [$^{18}$F], an aminooxy group was introduced by using the commercially available *N*-Boc-protected aminooxy acetic acid (Boc-Aoa-OH). A convenient way of radiolabeling PSMA analogs with [$^{18}$F] is using [$^{18}$F]FDG as a prosthetic group. The site-specific labeling was facilitated by the oxime bond formation between the N-terminal aminooxy group present in the PSMA backbone and the aldehyde group found in the open-chain form of [$^{18}$F]FDG. This has an added advantage as it combines both glycosylation and radiolabeling in one single step, which may be beneficial in improving the pharmacokinetic and tumor-targeting properties of the radiolabeled PSMA compounds. Nonetheless, our results demonstrated that the aminooxy-PSMA conjugates were radiolabeled efficiently with the [$^{18}$F] prosthetic group in the presence of a small amount of aniline as a nucleophilic catalyst [23]. Also, the DOTA-coupled PSMA conjugates showed high labeling efficiency when radiolabeled with [$^{68}$Ga] radionuclide under mild acidic conditions.

High metabolic stability is important for tumor-targeting biomolecules, as intact radioconjugates can deliver maximal tumor-targeting effects to tumor lesions. The in vitro stability of the [$^{68}$Ga/$^{18}$F]-labeled PSMA conjugates in human plasma was good, with low enzymatic degradation. In vitro, cell binding with PSMA-positive LNCaP cells indicated that the binding of [$^{68}$Ga/$^{18}$F]-labeled PSMA conjugates to prostate cancer cells was found to be saturable and receptor-specific. Nonetheless, variable degrees of binding affinities ($K_d$ varied from 39.92 ± 9.89 nM to 94.10 ± 13.78 nM) were observed with different [$^{18}$F]- and [$^{68}$Ga]-labeled PSMA conjugates. [$^{68}$Ga]Ga-DOTA PSMA-617 was evaluated as a reference along with the novel linker-modified PSMA ligands and showed a binding affinity value of 25.72 ± 4.84 nM. Significant effects on the binding affinity to PSMA were observed depending on the nature of linker modification. For example, the addition of Glu or Di-Phe linkers between the PSMA binding motif and the chelating agent resulted in nearly a two-fold decrease in affinity compared to the PSMA-617. Aoa-functionalized PSMA-617 showed somewhat lower affinity when compared with the corresponding DOTA-coupled PSMA-617 (39.92 nM vs. 25.72 nM). The PSMA ligands, comprising one linker, such as Ahx and Amb, showed the lowest affinity amongst the PSMA ligands evaluated in this study (Table 1). Interestingly, the bis-PSMA ligand exhibited a reasonably good affinity profile compared to the monomers. These binding data demonstrate that the bivalent conjugate is an attractive approach for enhancing tumor-targeting potential, possibly due to a synergistic increase in binding sites because of the presence of two binding motifs in the same construct.

In vivo, biodistribution and tumor targeting in LNCaP tumor xenografted mice demonstrate the suitable overall pharmacokinetic characteristics, such as the rapid clearance from blood and reasonably low uptake and retention by the kidneys. Additionally, a good tumor targeting potential of some of the PSMA conjugates, and in particular, bis-PSMA, can make it a potential candidate for targeting PSMA-positive prostate cancer in vivo. Even though the uptake in tumors was not very remarkable for any of the peptides tested, the amount of radioactivity found for the [$^{68}$Ga/$^{18}$F]-labeled PSMA conjugates in the LNCaP tumors was found to be always higher than the radioactivity present in the blood and muscle, resulting in good tumor to blood and tumor to muscle ratios. The results also emphasized the great influence of the linker groups in the PSMA scaffold on the binding and tumor targeting characteristics. The receptor-blocking dosage of PSMA reduces the uptake in the

 doi:10.20944/preprints202604.0979.v1



respective organs that express these receptors, and a varied pattern of impact from the dosage was noted in other tissues and organs. Findings from small animal PET imaging indicated a significant level of radioactivity concentrated in the kidneys and urinary bladder, although the implanted LNCaP tumors are still fairly detectable in the PET images. Considering these factors, the favorable tumor-targeting characteristics, combined with the promising pharmacokinetics of the bis-PSMA conjugate, suggest the potential of this radioligand for in vivo targeting of PSMA-positive tumors.

## 5. Conclusion

Seven new PSMA-based ligands were efficiently synthesized and tested for their PSMA targeting abilities in preclinical settings. Both in vitro and in vivo studies demonstrated that low-molecular-weight PSMA inhibitors, particularly the bis-PSMA conjugate under investigation, could effectively target PSMA-expressing LNCaP prostate cancer cells and tumor xenografts. The bis-PSMA homodimer approach has the potential to enhance prostate cancer targeting capability by increasing binding sites through synergism. The overall findings of this study, especially regarding the choice of a suitable linker group, could aid in developing more potent PSMA tracers for prostate cancer diagnosis. Additionally, further research is necessary to assess the true effectiveness of bis-PSMA probes in PET-based noninvasive diagnostic imaging of prostate cancer.

**Supplementary Materials:** The following supporting information can be downloaded at the website of this paper posted on Preprints.org.

**Funding:** This research project was supported by Innovation and Research, King Faisal Specialist Hospital and Research Centre.

**Institutional Review Board Statement:** All animal studies were conducted according to the international regulations governing the safe and proper use of laboratory animals. Approval for the animal protocol used in these studies was obtained from the Institutional Animal Care and Use Committee. The laboratory animals were received from the Jackson Laboratory, Bar Harbor, ME, USA. All the procedures and experiments involving laboratory animals were reviewed and approved by the Institutional Animal Care and Use Committees (IACUC) and Research Advisory Council (RAC; Project# 2250024) of the King Faisal Specialist Hospital and Research Centre (KFSH&RC). Animal housing, handling, and experimental procedures were conducted in the Association for Assessment and Accreditation of Laboratory Animal Care International (AAALAC) accredited laboratory animal facility at the KFSH&RC.

**Informed Consent Statement:** Not applicable.

**Data Availability Statement:** Data is contained within the article.

**Acknowledgments:** The author would like to thank Dr. Monther Alalwan for providing the cells; Celestina Maccuto for animal experiments, and Dr. Falah Mohanna for assistance in the induction of cancer cells in mice. The support of the Research and Innovation Administration is greatly acknowledged.

**Conflicts of Interest:** The authors declare no conflict of interest.

## References

1. Leslie, S.W.; Soon-Sutton, T.L.; Skelton, W.P. Prostate Cancer. 2024 Oct 4. In: StatPearls [Internet]. Treasure Island (FL): StatPearls Publishing; 2026 Jan. PMID: 29261872.
2. Okarvi, S.M. Recent developments of prostate-specific membrane antigen (PSMA)-specific radiopharmaceuticals for precise imaging and therapy of prostate cancer: an overview. *Clin Transl Imaging* **7**, 189–208 (2019). https://doi.org/10.1007/s40336-019-00326-3

 doi:10.20944/preprints202604.0979.v1




3. Debnath, S.; Zhou, N.; McLaughlin, M.; Rice, S.; Pillai, A.K.; Hao, G.; Sun, X. PSMA-Targeting Imaging and Theranostic Agents-Current Status and Future Perspective. Int J Mol Sci. 2022 Jan 21;23(3):1158. doi: 10.3390/ijms23031158. PMID: 35163083; PMCID: PMC8835702.
4. Wüstemann, T.; Bauder-Wüst, U.; Schäfer, M.; Eder, M.; Benesova, M.; Leotta, K.; Kratochwil, C.; Haberkorn, U.; Kopka, K.; Mier, W. Design of Internalizing PSMA-specific Glu-ureido-based Radiotherapeuticals. Theranostics. 2016 Apr 28;6(8):1085-95. doi: 10.7150/thno.13448. PMID: 27279903; PMCID: PMC4893637.
5. Rogers, O.C.; Rosen, D.M.; Antony, L. et al. Targeted delivery of cytotoxic proteins to prostate cancer via conjugation to small-molecule urea-based PSMA inhibitors. *Sci Rep* **11**, 14925 (2021). https://doi.org/10.1038/s41598-021-94534-5
6. Murce, E.; Beekman, S.; Spaan, E.; Handula, M.; Stuurman, D.; de Ridder, C.; Seimbille, Y. Preclinical Evaluation of a PSMA-Targeting Homodimer with an Optimized Linker for Imaging of Prostate Cancer. Molecules 2023, 28, 4022. https://doi.org/10.3390/molecules 28104022
7. Xie, Q.; Yang, J; Li, J.; Qin, J.; Tang, R.; Zhao, J.; Peng, Y.; Qiu, L.; Lin, J. Preclinical Evaluation Study of $^{68}$Ga-Labeled PSMA-Targeted Dimer Probe. Chem Biomed Imaging. 2025 Jul 10;4(1):54-63. doi: 10.1021/cbmi.5c00048. PMID: 41613756; PMCID: PMC12848698.
8. Hennrich, U.; Eder, M. [177Lu]Lu-PSMA-617 (PluvictoTM): The First FDA-Approved Radiotherapeutical for Treatment of Prostate Cancer. *Pharmaceuticals* 2022, *15* (10), 1292.
9. Geis, N.M.; Braunwarth, Y.; Meyer, P.T.; Eder, M, Eder AC. Optimizing PSMA-617-based inhibitors through charged linker modifications: Insights into structure-activity relationships. Theranostics. 2026 Jan 1;16(6):2798-2810. doi: 10.7150/thno.118972. PMID: 41510166; PMCID: PMC12775819.
10. Lundmark, F.; Olanders, G.; Rinne, S.S.; Abouzayed, A.; Orlova, A.; Rosenström, U. Design, Synthesis, and Evaluation of Linker-Optimised PSMA-Targeting Radioligands. Pharmaceutics. 2022 May 20;14(5):1098. doi: 10.3390/pharmaceutics14051098. PMID: 35631684; PMCID: PMC9147442.
11. Salih, S.; Elliyanti, A.; Alkatheeri, A.; AlYafei, F.; Almarri, B.; Khan, H. The Role of Molecular Imaging in Personalized Medicine. J Pers Med. 2023 Feb 19;13(2):369. doi: 10.3390/jpm13020369. PMID: 36836603; PMCID: PMC9959741.
12. Singh, D.; Dhiman, V.K., Pandey, M.; Sharma, A.; Pandey, H.; Verma, S.K.; Pandey, R. Personalized medicine: An alternative for cancer treatment, Cancer Treatment and Research Communications, Volume 42, 2024, 100860, ISSN 2468-2942, https://doi.org/10.1016/j.ctarc.2024.100860.
13. Benešová, M.; Bauder-Wüst, U.; Schäfer, M.; Klika, K.D.; Mier, W.; Haberkorn, U.; Kopka, K.; Eder, M. Linker Modification Strategies To Control the Prostate-Specific Membrane Antigen (PSMA)-Targeting and Pharmacokinetic Properties of DOTA-Conjugated PSMA Inhibitors. J Med Chem. 2016 Mar 10;59(5):1761-75. doi: 10.1021/acs.jmedchem.5b01210. Epub 2016 Mar 1. PMID: 26878194.
14. Huang, S.S.; Wang, X.; Zhang, Y.; Doke, A.; DiFilippo, F.P.; Heston, W.D. Improving the biodistribution of PSMA-targeting tracers with a highly negatively charged linker. Prostate. 2014 May;74(7):702-13. doi: 10.1002/pros.22789. Epub 2014 Feb 24. PMID: 24615708.
15. Benešová, M.; Schäfer, M.; Bauder-Wüst, U.; Afshar-Oromieh, A.; Kratochwil, C.; Mier, W.; Haberkorn, U.; Kopka, K. Eder, M. Preclinical Evaluation of a Tailor-Made DOTA-Conjugated PSMA Inhibitor with Optimized Linker Moiety for Imaging and Endoradiotherapy of Prostate Cancer. J Nucl Med. 2015 Jun; 56(6):914-20. doi: 10.2967/jnumed.114.147413. Epub 2015 Apr 16. PMID: 25883127.
16. Zia, N.A.; Cullinane, C.; Van Zuylekom, J.K.; Waldeck, K.; McInnes, L.E.; G. Buncic, G.; Haskali, M.B.; Roselt, P.D.; Hicks, R.J.; Donnelly, P.S. A Bivalent Inhibitor of Prostate Specific Membrane Antigen Radiolabeled with Copper-64 with High Tumor Uptake and Retention. Angew. Chem. Int. Ed. 2019, 58, 14991-14994. doi: 10.1002/anie.201908964. Epub 2019 Sep 5. PMID: 31437347.
17. Schäfer, M.; Bauder-Wüst, U.; Leotta, K.; Zoller, F.; Mier, W.; Haberkorn, U.; Eisenhut, M.; Eder, M. A dimerized urea-based inhibitor of the prostate-specific membrane antigen for 68Ga-PET imaging of prostate cancer. EJNMMI Res. 2012 Jun 6;2(1):23. doi: 10.1186/2191-219X-2-23. PMID: 22673157; PMCID: PMC3502552.
18. Martin, S.; Schreck, M.V.; Stemler, T.; Maus, S.; Rosar, F.; Burgard, C.; Schaefer-Schuler, A.; Ezziddin, S.; Bartholomä, M.D. Development of a homotrimeric PSMA radioligand based on the NOTI chelating

 doi:10.20944/preprints202604.0979.v1



platform. EJNMMI Radiopharm Chem. 2024 Dec 11;9(1):84. doi: 10.1186/s41181-024-00314-7. PMID: 39661209; PMCID: PMC11635053.

19. Nordquist, L.; Lengyelova, E.; Saltzstein, D.; Josephson, D.; Franklin, G.; Morrish, G.; Gervasio, O.; Parker, M.; Miller, R.; Shore, N. COBRA: Assessment of safety and efficacy of 64Cu-SAR-bisPSMA in patients with biochemical recurrence of prostate cancer following definitive therapy. Journal of Nuclear Medicine June 2024, 65 (supplement 2) 242291;
20. Gorin, M.A.; Lengyelova, E.; L.; Morrish, G.; Gervasio, O.; Miller, R.M.; Shore, N.D. CLARIFY: Positron emission tomography using $^{64}$Cu-SAR-bisPSMA in patients with high-risk prostate cancer prior to radical prostatectomy—A phase 3 diagnostic performance study. *J Clin Oncol* 43, TPS429 (2025). Vol. 43, No 5_suppl. DOI: 10.1200/JCO.2025.43.5_suppl.TPS429
21. Chan, W.; White, P. Fmoc solid phase peptide synthesis: A practical approach. Oxford Academic; 1999.
22. Okarvi, S.M.; Maliki, Y. Preparation and preclinical evaluation of $^{18}$F-labeled folate-RGD peptide conjugate for PET imaging of triple-negative breast carcinoma. EJNMMI Radiopharm Chem. 2025 May 19;10(1):25. doi: 10.1186/s41181-025-00349-4. PMID: 40389652; PMCID: PMC12089016.
23. Okarvi, S.M. A novel solid phase synthesis of an estradiol derivative and preclinical evaluation for targeting estrogen receptor positive breast cancer. Scientific Reports | (2025) 15:30143 | https://doi.org/10.1038/s41598-025-15367-0
24. Wendeler, M.; Grinberg, L.; Wang, X.; Dawson, P.E.; Baca, M. Enhanced catalysis of oxime-based bioconjugations by substituted anilines. Bioconjug Chem. 2014; 25:93–101.
25. Vegt, E, de Jong, M.; Wetzels, J.F.; Masereeuw, R.; Melis, M.; Oyen, W.J.; Gotthardt, M.; Boerman, O.C. Renal toxicity of radiolabeled peptides and antibody fragments: mechanisms, impact on radionuclide therapy, and strategies for prevention. J Nucl Med. 2010 Jul;51(7):1049-58. doi: 10.2967/jnumed.110.075101. Epub 2010 Jun 16. PMID: 20554737.